Th-AM-SymI-1

MULTISUBUNIT ASSEMBLY OF NICOTINIC AchR. ((L. Role)) Columbia Univ. Col. of P & S.

Th-AM-SymI-2

THE G PROTEIN-REGULATED INWARD RECTIFIER K^+ CHANNEL, GIRK1. ((D.E. Clapham)) Dept. Pharmacology, Mayo Foundation, Rochester, MN 55905.

Recent experiments to define G protein control of the cloned inwardly rectifying K^+ channel (GIRK1 or KGA) will be discussed.

Th-AM-SymI-3

GIRK CHANNELS. ((L. Jan)) Univ. of California at San Francisco.

Th-AM-SymI-4

CFTR GATING AND ATP HYDROLYSIS. ((D.C. Gadsby, T.-C. Hwang, G. Nagel, T. Baukrowitz, M. Horie & *A.C. Nairn)) Laboratories of Cardiac/Membrane Physiology and *Molecular and Cellular Neuroscience, The Rockefeller University, New York, NY 10021.

Modulation of cardiac CFTR channel gating by hydrolyzable and non-hydrolyzable ATP analogs demonstrates that (i) ATP is hydrolyzed at both of CFTR's nucleotide binding domains (NBDs), at one to open the channel and at the other to prompt channel closing, (ii) the NBDs are functionally distinct, (iii) their activity is differentially regulated by incremental phosphorylation of CFTR by PKA, but (iv) the NBDs interact. Comparison of mutation location with severity of cystic fibrosis disease, and mutagenesis studies of channel function, establish that ATP hydrolysis at NBD1 opens, and at NBD2 normally closes, CFTR channels. The NBD2 cycle resembles the GTP hydrolysis cycle of G proteins, in that ATP binding at NBD2 stabilizes an active conformation, the CFTR channel open state, and that stabilization is enhanced by 2-3 orders of magnitude when AMP-PNP binds instead of ATP, reflecting the low rate of AMP-PNP dissociation from NBD2. In the absence of ATP, PKA phosphorylated CFTR channels remain closed during exposure to AMP-PNP and yet, within a few sec of its washout, show the usual brief openings during exposure to ATP. Were AMP-PNP able to bind tightly to NBD2 in the closed channels, their subsequent opening by ATP should have resulted in prolonged channel openings. The observed brief channel openings indicate that the AMP-PNP binding site on NBD2 does not exist until ATP has been hydrolyzed at NBD1. The necessary interaction between the NBDs is regulated by the degree of channel phosphorylation. Partially phosphorylated CFTR channels (at sites that must be dephosphorylated by PPase 2A) have only NBD1 functional: they show brief openings in the presence of ATP and they fail to respond to AMP-PNP. But, fully phosphorylated channels (additionally phosphorylated at sites dephosphorylated by PPases other than 2A) have both NBDs functional: they have a higher P_o in the presence of ATP, and become locked open by ATP plus AMP-PNP. Orthovanadate, a P_i analog, also stabilizes the open state of CFTR channels, but does so regardless of their P_o or degree of phosphorylation, confirming that an ATP hydrolysis cycle at NBD1 is coupled to channel opening. Characterization of the nucleotide specificity of the hydrolysis cycles at the two NBDs is in progress. Supported by NIH and NYHA.

COMPUTER SIMULATIONS

Th-AM-A1

VIBE: A VIRTUAL BIOMOLECULAR ENVIRONMENT FOR INTERACTIVE MOLECULAR MODELING.* ((C. Cruz-Neira, T. A. DeFanti, R. Langley, R. Stevens, P. A. Bash)) University of Illinois, Chicago, Florida State University, and Argonne National Laboratory, Argonne, IL 60439

Virtual reality tightly coupled to high performance computing and communications ushers in a new era for the study of molecular recognition and the rational design of pharmaceutical compounds. We have created a Virtual Biomolecular Environment (VIBE) which consists of (1) massively parallel computing to simulate the physical and chemical properties of a molecular system, (2) the Cave Automatic Virtual Environment (CAVE) for immersive display and interaction with the molecular system, and (3) a high-speed network interface to exchange data between the simulation and the CAVE. This new capability enables molecular scientists to have a visual, auditory, and tactile experience with a chemical system, while simultaneously manipulating its physical properties by steering, in real-time, a simulation executed on a supercomputer. We demonstrate the characteristics of VIBE using an HIV protease cyclic urea inhibitor complex.

*This work is supported by the U.S. Department of Energy, Office of Health and Environmental Research, under Contract No. W-31-109-ENG-38.

Th-AM-A2

CONSTRAINED PROTEIN LATERAL MOTION IN THE ERYTHROCYTE PLASMA MEMBRANE. ((A. Boey and D. Boal)) Dept. of Physics, SFU, BC V5A 1S6 (Spon. by D. Boal)

Lateral diffusion of integral proteins in fluid membranes is an important transport mechanism. There are various constraints to the diffusion. In some cells, the cytoskeletal network is found to hinder the diffusion of proteins substantially. We present a model in which the cytoskeleton is treated as a network of polymer chains attached to a flat bilayer and the membrane protein is a hard hemisphere of radius R with center on the bilayer edge. It is found that the mean displacement of directed protein motion decreases with increasing sphere radius approximately as $\lambda = 5.9\ R^{-1.4}$ where λ and R are given in nm. Spheres of radius greater than 26nm are effectively corraled by the cytoskeleton.

Th-AM-A3

STABILITY OF FLUID MEMBRANE AGAINST HOLE FORMATION FROM MONTE CARLO SIMULATION

((J. C. Shillcock, D. H. Boal))
Simon Fraser University. BC V5A 1S6.
(Spon. by D. H. Boal)

We perform Monte Carlo simulations of a fluid membrane subject to an applied stress and allow the spontaneous formation of a hole. The hole is subject to an energy cost proportional to its perimeter. At zero stress the membrane is only stable against hole formation for line tensions greater than 5.10-21 J/nm. Below this line tension the hole grows spontaneously in an apparent first-order transition. This is less than the value extracted by Fromherz from sonication experiments in an analysis of membrane rupture, and may form an absolute limit of stability for fluid membranes. Near the transition point we analyse the scaling behaviour of the hole at zero and non-zero stress.

Th-AM-A4

A NEW APPROACH FOR STUDYING ION CHANNELS CONTAINING SUBCONDUCTANCE STATES.

((S. Jovanovic, R.A. Levis* K.G. Lynn))
Dept. of Physics, Brookhaven National Lab., *Dept. of Physiology, Rush Medical College.

A new approach for studying single channel currents containing multiple conductance levels is presented. It is based on the calculation and analysis of 2D amplitude histograms constructed from pairs of data points {s(n),s(n+M)}, i.e., the signal and its replica delayed by an appropriate constant M. This histogram contains characteristic peaks. The peaks on the main diagonal show the state levels, while the side peaks represent transitions between states. This method provides (1) a two dimensional image of transitions between states, (2) the likelihood of switching from any particular state to other states, and (3) identification of unallowed transitions between states. The following example illustrates the technique. We simulated a single channel current with four states according to the transition rate matrix R and the vector of state levels A. In this example the relationship between transition rates and the side peaks on the 2D histogram are visually obvious; unallowed transitions are also apparent. We discuss both the advantages and limitations of this technique as well as the conditions necessary for achieving reliable results.

$$R=\begin{bmatrix}0&0&2&1\\2&0&2&0\\1&2&0&2\\0&2&1&0\end{bmatrix} \qquad A=\begin{bmatrix}0\\4\\7\\9\end{bmatrix}$$

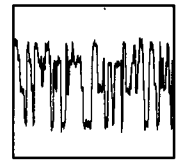

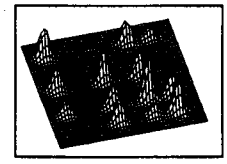

Th-AM-A5

THEORETICAL AND EXPERIMENTAL INVESTIGATIONS OF THE D-YSFUNCTIONS OF THE C.N.S USING NEURAL MODELING AND S-QUID MEASUREMENTS. ((A.G.Kotini and P.A.Anninos))Med-ical School,Democritus University of Thrace,Alex/pol-is Greece 68100.(Spon.by P.A.Anninos).

Using artificial neural nets of different laws of c-onnectivity with chemical markers it was investigated the conditions under which such nets exhibit epilept-ic features.Then it was applied non-linear dynamics and chaos in order to express the dynamics of these epileptic systems.The above findings were then compa-red with experimental data obtained using MEG measur-ement from epileptic patients.Furthermore in order to investigate,detect and quantitatively express any al-teration in the complexity underlying the dynamics of epileptic foci before and after the application of e-xternal magnetic fields,the correlation dimension of the existing strange attractors was estimated using chaotic analysis.The obtained results of dimensionali-ity estimation provides strong evidence for the exis-tence of strange attractors in the dynamics of epile-ptic foci.Finally the observed shift of the correlat-ion dimension derived from MEGs after the application of external magnetic fields on the localized foci and by other statistical analysis,indicate that the appl-ied magnetic fields affect the dynamics of neuronal epileptic foci in the brain.

Th-AM-A6

BURSTING, SPIKING, CHAOS, FRACTALS, AND UNIVERSALITY IN BIOLOGICAL RHYTHMS.

((T.R. Chay and Y.S. Lee)) Department of Biological Sciences, University of Pittsburgh, Pittsburgh, PA 15260.

Biological systems offer many interesting examples of oscillations, chaos, and bifurcations. Oscillations in biology arise because most cellular processes contain feedbacks that are appropriate for generating rhythms. These rhythms are essential for regulating cellular function. In this work, we treat two interesting nonlinear dynamical processes in biology that give rise to bursting, spiking, chaos, fractals, and universality: endogenous electrical activity of *excitable cells* and Ca^{2+} releases from the Ca^{2+} stores in *non-excitable cells* induced by hormones and neurotransmitters. We will first show that each of these complex processes can be described by a simple, yet elegant mathematical model. We then show how to utilize bifurcation analyses to gain a deeper insight into the mechanisms involved in the neuronal and cellular oscillations. With the bifurcating diagrams, we explain how spiking can be transformed to bursting via a complex type of dynamic structure when the key parameter in the model varies. Understanding how this parameter would affect the bifurcating structure is important in predicting and controlling abnormal biological rhythms, such as epileptic seizures. Although we describe two very different dynamic processes in biological rhythms, we will show that there is universality in their bifurcation structures.

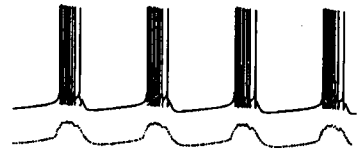

Th-AM-A7

COMPOSITION OF FUNCTIONS IN SOLVING SYSTEMS OF MULTIVARIATE HETEROGENEOUS EQUATIONS.

(Alafuele Mbuyi-Kalala) Biophysics Section, Clinical Neuroscience Branch, NINDS, NIH, Bethesda, MD 20892)

In the mathematical formulation of physical, chemical, and biological problems, more often than not systems of multivariate heterogeneous equations (of the type dX/dA = f [X(A), Z(A), U(A), K], where K is a set of constants and X, Y, Z, and U are functional variables of A) are obtained. Apart from the sheer number of variables, which fortunately can be in a good number of cases reduced with recourse to conservation equations or other state equations, the integration of these systems, i.e., the finding of analytical solutions, is generally unfeasible due to the presence of "non-directly related variables", e.g., Z(A) and U(A) in the above formulation. We show that the composition of functions can help homogenize these systems and thereby facilitate the search for analytical solutions. We illustrate this finding with a search for the analytical solutions to the Henri/Michaelis-Menten model and to the radioimmunoassay model.

Th-AM-B1

IMAGING FREE ZINC IN SYNAPTIC TERMINALS IN LIVE HIPPOCAMPAL SLICES.

((T. Budde, A. Minta[†], J.A. White, C.J. Frederickson[*], A.R. Kay))
Biol. Sci., Univ. of Iowa, Iowa City,IA 52242, [†]Texas Fluorescence Laboratories, Austin, TX 78747, [*]Lab. for Neurobiol. Univ. of Texas at Dallas, Richardson, TX 75080. (Spon. C.C.Wunder)

A high concentration of free zinc in synaptic vesicles is a prominent feature of some of the excitatory pathways in the mammalian cortex. A newly synthesized Zn-sensitive fluorescent probe, TFLZn (TEFLABS) was used to monitor intracellular zinc in live rat hippocampal slice. Slices were illuminated with a pulsed laser (337 nm, 3 ns) and imaged on an intensified CCD camera. Loading of slices with TFLZn (K^+ Salt, 0.25 mM) clearly delineated the mossy fiber (MF) pathway and terminals. Fluorescence intensity diminished after addition of kainate (10 μM) and 4AP (1 mM) to the bath, consistent with activity dependent release of Zn. Stimulation of the mossy fiber pathway (10 Hz) lead to release of Zn, that was blocked by TTX and low extracellular Ca .

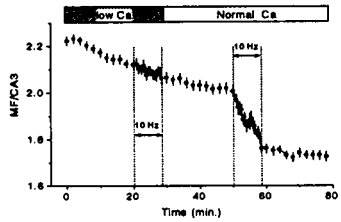

MF/CA3 = fluorescence intensity of MF/CA3 cell bodies (low Zn). Ext. soln. (mM): NaCl 124, KCl 4, $CaCl_2$ 3, $MgCl_2$ 2, $NaHCO_3$ 26, EDTA 1, D-glucose 10; pH 7.4. Slice preloaded with TFLZn (0.25 mM). Low Ca - 0.25 $CaCl_2$, 3.75 $MgCl_2$

Supported by grants from NIH-BRSG (CJF), NIH and ONR (ARK).

Th-AM-B2

The homeostasis of the vesicle pool in CNS synapses. T. A. Ryan and S. J Smith. Department of Molecular and Cellular Physiology, Stanford University, Stanford CA , 94305.

Using fluorescent optical tracer methods and quantitative microscopy we have characterized several important properties of the releasable synaptic vesicle pool in synaptic terminals of hippocampal neurons in culture. We have measured the size of the releasable pool of vesicles in individual synaptic boutons and shown that at a stimulus frequency of 10 Hz 90 % of the pool of vesicles is utilized within ~60 s. We have further characterized the dynamics of the replenishment of this releasable pool and shown that under these stimulation conditions the endocytic phase of vesicle recycling lags exocytosis by ~ 30 s and that a further 30 s is required for repriming before vesicles are competent for release. Finally we have shown that once vesicles have undergone this repriming period they are randomly mixed with vesicles which have not yet been released and compete equally with these for subsequent release upon the invasion of an action potential within the presynaptic terminal.

Th-AM-B3 *(Presented at Th-AM-E9 — Heme Proteins)*

HEME COORDINATION OF NO RESULTS IN THE INHIBITION OF NO SYNTHASE ((Jianling Wang*, Husam M. Abu-Soud#, Dennis J. Stuehr#, and Denis L. Rousseau*)) *AT&T Bell Laboratories, Murray Hill, NJ 07974, USA; #The Cleveland Clinic, Cleveland, OH 44195, USA;

A current question in nitric oxide biology is whether NO can act as a feedback inhibitor of NO synthase (NOS), which catalyzes the formation of NO from O_2 and arginine (Arg). Here we report evidence for the reversible binding of NO to the heme of NOS and the inhibition of the enzyme's function through this binding. Under an inert atmosphere NO coordinates to the heme of NOS, giving rise to Soret and visible absorption bands at 436 nm and 567 nm in the Fe^{2+}-NO complex, and at 440 nm and 548 and 580 nm in the Fe^{3+}-NO adduct, respectively. In the resonance Raman spectra the Fe-NO stretching ($\nu_{Fe\text{-}NO}$) mode is evident at 540 cm^{-1} in the ferric enzyme. In its ferrous adduct, the binding geometry of Fe-N-O depends critically on the presence of Arg ($\nu_{Fe\text{-}NO}$: 536 and 549 cm^{-1} in the absence and presence of Arg, respectively), suggesting that Arg binds directly over the heme and interacts with heme-bound ligands. In the absence of exogenous NO, NO synthesized by the neuronal NOS coordinated to the heme and formed a spectrally detectable Fe^{2+}-NO species, which caused a concomitant inhibition of most of the enzyme 's function. The effects of other inhibitors such as arginine analogs on the structural and functional properties of NOS will also be discussed. (J.Wang is supported by a grant from Nitional Institute of Health).

Th-AM-B4

DIFFERENTIAL MODULATION OF CORTICAL SYNAPTIC ACTIVITY BY CALCINEURIN (PHOSPHATASE 2B) VS. PHOSPHATASES 1 AND 2A.

((G.D. Thomas, R.G. Victor, E. Marban, B. O'Rourke)) Johns Hopkins Univ, Baltimore, MD 21205 and UT Southwestern Medical Ctr, Dallas, TX 75235

Recently, phosphatases (PP) 1, 2A, and 2B all have been shown to modulate synaptic neurotransmission. Our demonstration that specific calcineurin (PP 2B) inhibitors, cyclosporine (CsA) and FK506, act presynaptically to enhance spontaneous glutamatergic responses in cultured rat cortical neurons prompted closer study of the mechanism of action of calcineurin and other phosphatases. Using whole-cell voltage clamp with tetrodotoxin (TTX, 5 μM) to block spontaneous presynaptic depolarizations, we recorded miniature excitatory postsynaptic currents (minis) to determine if spontaneous vesicle release is modulated by calcineurin. In the presence of TTX, CsA had no effect on the frequency or amplitude of the minis (n=6), but, after TTX washout, CsA greatly increased the frequency of the large postsynaptic glutamatergic currents, indicating that calcineurin modulates excitation-secretion coupling rather than spontaneous vesicle release. In contrast to calcineurin inhibition, inhibition of PP 1 and 2A (but not 2B) with calyculin A (1 μM in bath solution) increased the amplitude of postsynaptic glutamatergic currents by 30% without altering their frequency (n=5). The increased current amplitude involved a postsynaptic mechanism, since the effect was reproduced by the membrane impermeant PP 1/2A inhibitor microcystin (10 μM in pipette solution, n=3). Calcineurin inhibition evoked an increase in the frequency of currents even after prior inhibition of PP 1 and 2A. Thus, in rat cortical neurons, glutamatergic neurotransmission is frequency-modulated through a presynaptic mechanism by calcineurin, and amplitude-modulated through a postsynaptic mechanism by phosphatases 1 and/or 2A.

Th-AM-B5

PRESYNAPTIC MODULATION OF CORTICAL SYNAPTIC ACTIVITY BY CALCINEURIN.

((R.G. Victor, G.D. Thomas, E. Marban, B. O'Rourke)) Johns Hopkins Univ, Baltimore, MD 21205 and UT Southwestern Med Ctr, Dallas, TX 75235

Recent evidence suggests that calcineurin, the Ca^{2+}-calmodulin dependent phosphatase (2B), modulates the activity of postsynaptic glutamate receptors when applied to excised patches. However, in rat cortex calcineurin is enriched mainly in presynaptic, not postsynaptic, fractions. To determine if calcineurin modulates glutamatergic neurotransmission through a presynaptic mechanism, we used whole cell patch-clamp to test effects of two specific calcineurin inhibitors, cyclosporine A (CsA) and FK506, on synaptic activity in fetal rat cortical neurons, which form glutamatergic synapses in primary culture. In current clamp experiments, CsA (5-10 μM) induced a 205% increase in the rate of spontaneous action potential firing (0.56±0.1 to 1.71±0.55 Hz, mean ±SE, n=4, $P<0.05$), while the solvent (γ-cyclodextrin) was without effect. Action potential firing was increased similarly with FK506 (0.5-1.0 μM, n=6) but was unaffected by rapamycin (0.5-5.0 μM, n=4), a structural analog of FK506 which has no effect on calcineurin. In voltage clamp experiments, (V_H -60mV), CsA (10 μM) increased the spontaneous rate but not the amplitude of excitatory postsynaptic glutamate receptor currents, suggesting an increased rate of glutamate release. Further evidence for a pre- rather than post- synaptic site of action is that CsA had no effect on the amplitude of currents evoked by brief bath application of selective glutamate receptor agonists, AMPA (936±154 vs. 887±181 pA, control vs. CsA, n=3) or NMDA (833±205 vs. 935±193 pA, n=4). We conclude that calcineurin modulates glutamatergic neurotransmission in rat cortical neurons through a novel presynaptic mechanism.

Th-AM-B6

CALCIUM ENTRY DURING THE REPOLARIZATION PHASE OF THE PRESYNAPTIC ACTION POTENTIAL SYNCHRONIZES THE ONSET OF POST-SYNAPTIC CURRENTS ((B. Yazejian, D. DiGregorio, A.D. Grinnell and J.L. Vergara)) Department of Physiology, UCLA, Los Angeles, CA 90024

We applied patch clamp techniques in cultured *Xenopus* neuromuscular junctions to investigate the role of ionic conductances in determining the shape of the presynaptic action potential and in mediating transmitter release. Simultaneous recordings were made from the soma, presynaptic terminal and postsynaptic myocyte. Sodium-dependent action potentials initiated at the cell body elicited broader action potentials at the presynaptic terminal which showed a pronounced after-hyperpolarization, often followed by a subsequent small depolarization. The onset of the end-plate currents (EPCs) was invariably synchronized with the falling phase of the presynaptic action potential. To understand the mechanism of this synchrony, we voltage-clamped presynaptic terminals in the absence of sodium and potassium conductances with action-potential-like command signals. We found that net inward calcium currents were only detectable after the peak, and predominantly during the falling phase, of the command voltage. Subsequent EPCs closely correlated in time with these inward currents. Furthermore, to investigate which ionic conductances participate in the repolarization phase of presynaptic potentials, we performed current-clamp experiments with K-channel blockers and found that a Ca-activated-K conductance (gK_{Ca}), sensitive to charybdotoxin, is the major repolarizing conductance. We propose that gK_{Ca} plays a key physiological role in synaptic transmission by forcing the repolarization of the presynaptic action potential and thus driving the entry of Ca^{2+} ions to synchronize presynaptic and postsynaptic electrical signals. Supported by NIH NS 30673 (ADG) and AR25201 (JLV).

Th-AM-C1

O_2-SENSITIVE Ca^{2+} CHANNELS IN SMOOTH MUSCLE AND THEIR ROLE IN HYPOXIC ARTERIAL RELAXATION. ((A.Franco, J.Ureña and J.López-Barneo)) Dept. Fisiol. Méd. Biofís. Universidad de Sevilla. 41009 Sevilla. Spain.

Hypoxia is an important local factor in the regulation of arterial tone. However, the responses of arterial myocytes to lowered environmental oxygen tension (PO_2) are poorly understood. We have examined the modifications of cytosolic [Ca^{2+}] and membrane Ca^{2+} permeability through voltage-gated channels by low PO_2. Fura-2 loaded arterial myocytes exhibit rhythmical oscillations of $[Ca^{2+}]_i$ which are reversibly suppressed by low PO_2. Adding 1 μM nifedipine to the bath interrupts the oscillations, while depolarizing myocytes with 30 mM K^+ increases their frequency. These observations suggest that the influx of Ca^{2+} through L-type Ca^{2+} channels influences the frequency of the oscillations. We therefore tested the possibility that macroscopic Ca^{2+} currents in arterial myocytes could be regulated by O_2 tension. Whole-cell patch clamped myocytes exhibit both T and L-type components of Ca^{2+} current. Exposure of the myocytes to physiologically relevant levels of hypoxia (between 145 and 20 mmHg) reversibly inhibits the L-type component of the Ca^{2+} current, whereas the T-type component is unaffected. The inhibition of L-type Ca^{2+} channels by hypoxia is strongly voltage-dependent. It is ~40% with voltage pulses to 0 mV (from a holding potential of -80 mV), although only ~2% with pulses to +20 mV. These results suggest that O_2-sensitive Ca^{2+} channels may have a key role in regulating arterial tone.

Th-AM-C2

DISTINCT DISTRIBUTION OF TS28 AND THE α_1 SUBUNIT OF THE 1,4-DIHYDROPYRIDINE RECEPTOR (α_1-DHPR) IN TRANSVERSE (T) TUBULES OF DEVELOPING RABBIT SKELETAL MUSCLE. (★A.O. JORGENSEN,★A.C.-Y. SHEN, AND ◇K.P. CAMPBELL) ★Dept. of Anatomy & Cell Biology, Univ. of Toronto, Toronto, Canada, M5S 1A8 & ◇HHMI, Dept. Physiol. & Biophysics, Univ. of Iowa, Iowa City, IA 52242, U.S.A.

The DHPR and TS28 are densely distributed in T-tubular membranes of adult skeletal muscle as determined by indirect immunoelectron microscopical labeling. To determine whether these two proteins are uniformly distributed in the T-tubular membrane or confined to either the junctional or the nonjunctional region of the T-tubular membrane, the same technique was used to determine their subcellular distribution in developing skeletal muscle (2 d old rabbit psoas muscle). This stage of development is very suitable for determining whether the DHPR and TS28 are present in junctional and/or nonjunctional T-tubules because forming T-tubules are arranged in an extensive branching network that only form occasional focal junctional complexes with junctional sarcoplasmic reticulum (SR).

The results strongly support the conclusion that TS28 is confined to the nonjunctional domain of T-tubules while the α_1-DHPR is confined to the region of the junctional complex between T-tubules and junctional SR. They also support previous immunofluorescence studies suggesting that α_1-DHPR and TS28 travel to their target domains of T-tubules via distinct intracellular pathways. (Supported by MRC of Canada.)

Th-AM-C3

THE ENHANCEMENT OF Ca^{2+} CHANNEL ACTIVITY BY TRYPSIN PERFUSION IS DUE TO PARTIAL REMOVAL OF THE C-TERMINAL TAIL OF THE α_1 POLYPEPTIDE ((U. Klöckner, G. Mikala, M. Varadi, G. Varadi and A. Schwartz)) University of Cologne, 50831 Cologne, Germany and University of Cincinnati, Cincinnati, OH 45267 (Spon. D. W. Behnke)

Intracellular dialysis of cardiac and vascular smooth muscle cells with trypsin enhances the amplitude of the calcium channel current several fold, most likely due to an increase in availability of the calcium channels. In order to characterize the underlying mechanism, we studied the effect of trypsin on the human cardiac L-type calcium channel in transiently transfected HEK293 cells. Perfusion of 1 mg/ml trypsin in transfected cells expressing hHTα_1, skα_2 and hβ_3 resulted in about a 3 fold increase in the peak amplitude of the calcium channel current within 5-10 min (40 mM Ba^{2+} as charge carrier, 22°C). Simultaneously with the increase in I_{Ba}, a reduction of inactivation time course of the calcium channel current was observed. No shift of the voltage dependence of the calcium channel current was found. Similar results were obtained in HEK cells expressing only hHTα_1 alone, suggesting that the α_2 and β subunits are not involved in the action of trypsin. Expression of carboxyterminal deletion mutants until aa 1633 in HEK cells, directed calcium channel currents with about 3 fold higher current density and faster inactivation time compared to the wild type. Trysin perfusion of these cells did not cause an increase but only a decrease of I_{Ba}.

We conclude: (1) the C-terminal tail of the calcium channel α_1 subunit is the primary target for protease action; the effects of trypsin are also detectable in the absence of β subunits (2) the C-terminal tail region of the α_1 polypeptide inhibits channel activity (3) the C-terminal tail region is likely to be a component of the inactivation machinery of the channel.

Th-AM-C4

DEPOLARIZATION SHIFTS THE VOLTAGE DEPENDENCE OF CARDIAC SODIUM CHANNEL AND CALCIUM CHANNEL GATING CHARGE MOVEMENTS. ((I.R. Josephson)) Department of Molecular and Cellular Physiology, University of Cincinnati, College of Medicine, Cincinnati, OH 45267-0576.

In cardiac ventricular myocytes, membrane depolarization leads to inactivation of Na channel and Ca channel ionic currents. The inactivation of the ionic currents has been associated with a reduction of the gating charge movement ("immobilization") which governs the activation of Na channels and Ca channels. The nature of the apparent "immobilization" of the charge movement following depolarization of embryonic chick ventricular myocytes was explored using voltage protocols applied from depolarized holding potentials. It was found that nearly all of the charge was still mobile following inactivation, but that the voltage dependence of its movement was shifted to more negative potentials. In addition, the shift in the distribution of the Na channel charge could be differentiated from that of the Ca channel charge on the basis of kinetic, as well as steady-state criteria. These results suggest that the voltage-dependent activation of Na channel and Ca channel charge movements leads to conformational changes and charge rearrangements that differentially bias the movements of the Na channel and Ca channel voltage sensors, and concomitantly produce channel inactivation. Supported by the NIH.

Th-AM-C5

REGULATION OF RECOMBINANT N-TYPE Ca CHANNELS BY G-PROTEINS AND VOLTAGE ((P. Patil, M. de Leon, R. Reed, S. Dubel*, T.P. Snutch*, and D.T. Yue)) Johns Hopkins U. Sch. Medicine, Baltimore MD & U. British Columbia, Vancouver, BC*

N-type Ca channels play a critical role in the control of synaptic transmission. Potent regulatory mechanisms for the channel include voltage-dependent inactivation and G-protein inhibition. Here we reconstitute these mechanisms in HEK 293 cells co-transfected with α_{1B} β_{1b}, and α_2 Ca channel subunits. In pre-pulse inactivation protocols, test-pulse current manifests a U-shaped dependence upon pre-pulse voltage (*Vp*). With 300 μM internal GDP-βS, inactivation is most prominent for $Vp \approx 20$ mV and is insignificant below -30 mV and above 100 mV. Inactivation is identical with Ba, Ca, or Li as the permeant ion, arguing that this is a voltage-dependent, not current-dependent, phenomenon. With 300 μM internal GTP-γS, there is a marked facilitation of test-pulse current for $Vp > 50$ mV (**A**, 10 mM Ba), indicating reconstitution of N-type Ca channel inhibition by endogenous G proteins. Notably, the popular candidate for G-protein inhibition, G_o, is not found in HEK 293 cells. One provocative proposal for G-protein inhibition is that permeation, and not only gating, is modulated. Key support includes diminished facilitation for monovalent vs. divalent cations (Kuo & Bean, *Nature*, 1993). We re-examine this question, but in a pure population of N-type Ca channels. Facilitation is appreciably diminished when Li substitutes for Ba (**B**, 140 mM Li). Reconstitution of these regulatory mechanisms opens the door to molecular analysis of channel behavior and regulation in a pure population of N-type Ca channels.

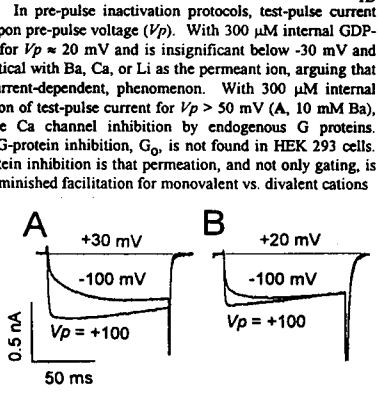

Th-AM-C6

THREE L-TYPE Ca CHANNELS (FROM ~3000) CARRY THE STEADY CA CURRENT IN SMOOTH MUSCLE CELLS FROM RESISTANCE ARTERIES. ((M. Rubart, J. Patlak, and M. T. Nelson)) Depts. of Pharmacology and Physiology, University of Vermont, Burlington, VT 05405)

We hypothesize that the degree of Ca channel activation at physiological extracellular Ca concentration (2 mM) and membrane potential (-40 mV) is sufficient to provide enough intracellular Ca to sustain arterial tone. We sought to quantify the total steady Ca current, as well as the number of channels responsible for its flow, by measuring both single channel and whole cell currents through dihydropyridine - sensitive Ca channels. Smooth muscle cells were freshly isolated from rat posterior cerebral arteries (100 μm diameter). The peak whole cell Ca currents ($I = N*i*Po$) in response to depolarized pulses were -52 ± 5 pA, increasing to -112 ± 21 pA (N=5) in the presence of 500 nM BayK8644. The unitary current amplitude, i, at -40 mV was -0.19 pA, with a slope conductance of 3.5 pS over the potential range of -70 to -20 mV. Unitary currents at more depolarized potentials were estimated by fitting the i-V curve. We thus estimated $I/i = N*Po$ as a function of voltage (i.e. the activation curve), indicating that the whole cell currents during such pulses were carried by, at minimum, about 3000 channels.

Cobalt sensitive steady - state Ca currents were measured in the whole cell configuration in the presence of 130 mM intracellular Cs and 142 mM extracellular TEA to block potassium currents. These currents were -0.23 ± 0.04, -0.42 ± 0.04, and -0.79 ± 0.1 pA at -40, -30 and -20 mV, respectively, corresponding to 29%, 25% and 18% of their respective peak currents elicited during voltage steps to the same potentials. The number of channels open *on average* at these steady holding potentials (-40, -30, and -20 mV) was 1, 3, and 7, respectively. Our results show that 1-5 channels (of at least 3000 that are present in a cell) are simultaneously open on average in a single smooth muscle cell at physiological membrane potentials. Fleischmann et al. (PNAS, in press) have recently provided evidence that a half pA of steady Ca influx should be sufficient to elevate free intracellular Ca. We propose therefore that the steady Ca currents through a handful of channels are sufficient to explain the maintained tone in resistance arteries. *Supported by NSF, NIH, and the Krannert Institute of Cardiology.*

Th-AM-C7

HIGH AND LOW AFFINITY LOCAL ANESTHETIC BINDING SITES ON NEURONAL CALCIUM CHANNELS ((G.W. Zamponi, E. Bourinet and T.P. Snutch)) Biotechnology Laboratory. University of British Columbia. Vancouver, Canada, V6T 1Z3.

The local anesthetic bupivacaine has been previously shown to block voltage-gated calcium channels (i.e. Sanchez-Chapula. 1988. Eur. J. Pharmacol. 156: 303). Here, we report block of cloned neuronal α_{1A}, α_{1C}, and α_{1E} calcium channels expressed in Xenopus oocytes by flecainide, a class I antiarrhythmic, and fomocaine, a local anesthetic. Both compounds share with bupivacaine a tertiary amine as part of a piperidine (fomocaine, bupivacaine) or morpholine (fomocaine) ring. Fomocaine was most effective with α_{1E} channels ($K_d \approx 100$ μM), while block of α_{1A} and α_{1C} occurred, respectively, with 4 and 10-fold lower affinity. Flecainide also showed the greatest affinity for α_{1E} ($K_d \approx 300$ μM). Block by either compound was only partially reversible upon washout, appeared to follow 1:1 kinetics, and was weakened upon increasing the external barium concentration, suggesting that the blocking site is confined to a part of the channel which is exposed to the aqueous solution such as the narrow region of the pore. In contrast, the uncharged compound piperazine had no effect. Procaine and diethylcarbamazine (an essentially permanently charged hybrid between procaine and piperazine) both blocked with low affinity ($K_d \approx 2$ to 5 mM). However, block was readily reversible upon washout and did not show a preference for α_{1E}. Furthermore, in a series of experiments with α_{1A}, diethylcarbamazine appeared to compete with procaine, but not with fomocaine, suggesting the presence of two distinct blocking sites on some types of neuronal calcium channels; a low affinity binding site accessible directly from the extracellular side which presumably interacts with simple tertiary amines, and a second site, which may act via the cytoplasmic side and which interacts with tertiary amines which are part of piperidine or morpholine rings. Our results suggest that the second site may control the subtype specificity of fomocaine and flecainide block, and perhaps a range of piperidine antipsychotics and antiepileptics thought to preferentially block low threshold calcium channels (Enyeart et al., 1992. Mol. Pharmacol. 42: 364).

Th-AM-C8

cAMP-DEPENDENT PHOSPHORYLATION SITES ARE NOT REQUIRED FOR ACTIVITY OF THE RECOMBINANT CARDIAC L-TYPE CALCIUM CHANNEL. ((G. Mikala, U. Klöckner, J. Eisfeld, M. Varadi, G. Varadi and A. Schwartz)) University of Cincinnati, Cincinnati OH 45267 and University of Cologne, Cologne, Germany (Spon. by A. Schwartz)

The importance of cAMP-dependent phosphorylation sites for activity of the cardiac L-type calcium channels was studied by site-directed mutagenesis followed by recombinant expression in HEK293 cells. Mutagenesis of serine residues of the individual PKA consensus phosphorylation sites resulted in L-type calcium channel currents and receptor function for calcium channel antagonists that were indistinguishable from the wild type channel. The removal of 2 or 3 phosphorylation sites by deleting a 507 or 547 amino acid long region from the C-terminal tail of the α_1 polypeptide to amino acids 1673 and 1633, resulted in a 3-fold increase in current density and a 50-70% acceleration of inactivation. Removal of all of the PKA phosphorylation sites at the C-terminal tail **by deletion** up to aa 1500 resulted in a complete loss of the channel and drug receptor functions. However, removal of all PKA consensus sites **by simultaneous point mutations** (Ser to Ala) did not alter current density, kinetic parameters and calcium antagonist receptor function compared to wild type. We conclude that cAMP-dependent phosphorylation sites are not required for activity of the cardiac L-type calcium channels. Moreover, all of our experiments to date are indicative that phosphorylation of the channel in HEK293 cells has no effect. In this sense, this system behaves very similar to vascular smooth muscle in that PKA phosphorylation plays no role in regulation of the L-type voltage-dependent calcium channel.

Th-AM-C9

A STRUCTURAL ROLE FOR THE β SUBUNIT IN THE ASSEMBLY OF FUNCTIONAL L-TYPE VDCC'S. ((G. Varadi, U. Klöckner, M. Varadi, G. Mikala and A. Schwartz)) University of Cincinnati, Cincinnati, OH 45267 (Spon. K. Itagaki)

Functions of α_1 subunits for various voltage-dependent calcium channels are modulated by β subunits. The most consistently appearing consequences of α_1-β interaction are increase in current density and increase in drug/toxin binding sites. Translation of human cardiac α_1 together with α_2 and β subunit cRNAs in a cell-free translation system did not result in enhanced total incorporation into polypeptides when all subunits were simultaneously present. However, a dramatic enhancement in translational accuracy was observed when the subunit cRNAs were cotranslated in the presence of canine pancreatic microsomes. This effect occurs whether α_1 was translated alone or in combination with other subunits. Additionally, a 2-fold increase in amino acid incorporation into the full length α_1 polypeptide was observed when α_1 and β messages were cotranslated. Resistance to protease digestion showed a similar pattern for membrane protected peptide fragments regardless whether α_1 was translated alone or in combination with other subunits. We conclude that the primary function of the β subunit is to facilitate the oligomerization process of the complex. Further, we feel that the appropriate complex of subunits is required for vesicular targeting and transport from the endoplasmic reticulum to the plasma membrane.

Th-AM-C10

COEXPRESSION OF β SUBUNIT WITH L-TYPE CALCIUM CHANNEL α_{1C} SUBUNIT IN HEK 293 CELLS INCREASES IONIC AND GATING CURRENTS. ((T. J. Kamp, M. T. Perez-Garcia, and E. Marban)) Division of Cardiology, Dept. of Medicine, Johns Hopkins University, Baltimore, MD 21205.

Coexpression of the β subunit with the α_{1C} subunit of the L-type Ca channel in mammalian cell lines has previously been shown to increase both the density of macroscopic current and dihydropyridine binding sites. The present study examines the basis for the β subunit modulation by characterizing the gating currents associated with the expressed channels. HEK293 cells were transfected with a plasmid encoding the rabbit cardiac Ca channel α_{1C} subunit with or without a plasmid encoding the rabbit skeletal muscle Ca channel β subunit. Peak inward Ba^{2+} current (I_{Ba}) at 0 mV was increased by β subunit coexpression from 10.2±3.5 to 42.4±13.4 pA/pF (10 mM Ba). After blocking the ionic currents with 100 μM Cd and 100 μM La and subtraction of the linear capacitative current, gating currents were detected only in transfected cells. The measured gating charge movement was nonlinear and could be described by a Boltzmann distribution with the charge movement at the beginning of the test pulse approximating the charge movement at the end of the test pulse. This charge movement was immobilized over a similar voltage range as inactivation of I_{Ba} and was blocked by 10 μM nitrendipine. The primary effect of coexpression of the β subunit on the measured charge movement was to increase the density of charge movement (Q_{max}) from 2.7±0.6 to 7.56±1.1 fQ/pF. These results suggest that β subunit coexpression results in more functional channels in the surface membrane.

MEMBRANE FUSION: EXOCYTOSIS AND ENDOCYTOSIS II

Th-AM-D1

ENERGETICS OF LIPID INTERMEDIATES IN PROTEIN-MEDIATED MEMBRANE FUSION: MECHANISTIC IMPLICATIONS. ((D. P. Siegel)) Procter & Gamble Co., P.O. Box 398707, Cincinnati, OH 45239-8707.

Calculations using a model for the energies of lipid fusion intermediates indicate that fusion in uncharged or sparsely-charged lipid systems probably occurs via a stalk/TMC mechanism [1]. Here this model is used to determine how fusion proteins could lower the activation energy (catalyze formation) of lipidic fusion intermediates. It is shown that proteins could lower the minimum activation energy by ca. 50% simply by making amphipathic moieties and hydrophobic transmembrane domains available at the proper locations. However, fusion proteins may act by a qualitatively different type of mechanism. For instance, fusion-relevant conformational changes in proteins like influenza HA are profound [2] and liberate large amounts of energy [3], implying that proteins may play a more central role in the mechanism. Here it is shown that if a fusion protein acts by a simple modification of the stalk/TMC mechanism, then the fusion rate should exhibit four specific types of behavior as a function of lipid composition. Thus, results of fusion rate measurements in reconstituted systems or in native systems with different target membranes can be used to determine the relevant type of mechanism. It is also shown that membrane rupture tension, not considered in [1], may affect membrane fusion rates.
[1] Siegel, Biophys. J. 65:2124 [1993]; [2] Bullough et al., Nature 371:37 [1994]; [3] Remeta et al, Biophys. J. 66:A177 [1994].

Th-AM-D2

COMPUTER SIMULATION OF THE FUSION INHIBITING PEPTIDE Z-D-PHE-PHE-GLY BOUND TO N-ME-DOPE BILAYERS ((K. V. Damodaran and Kenneth M. Merz Jr.)) Department of Chemistry, 152 Davey Laboratory, The Pennsylvania State University, University Park, Pennsylvania 16802.

We have carried out simulations that examine the binding of the fusion inhibiting peptide (FIP) Z-D-Phe-Phe-Gly to an N-Me-DOPE based lipid bilayer. From computed order parameter profiles we find that this FIP causes an ordering of the upper portion of the alkyl region of the bilayer, while the interior region experiences an increase in disorder. Furthermore, we find that the FIP dehydrates the head-group region of the lipid bilayer. From these observations we postulate that the dehydration and ordering effects are responsible for the observed antifusogenic capabilities of this peptide.

Th-AM-D3

MEMBRANE ORIENTATION OF THE SIV FUSION PEPTIDE DETERMINES ITS EFFECT ON BILAYER STABILITY AND ABILITY TO PROMOTE MEMBRANE FUSION. ((R.F. Epand[†], I.Martin[‡], J.-M. Ruysschaert[‡] and R.M. Epand[†])) [†]Dept. of Biochemistry, McMaster University, Hamilton, ON, L8N 3Z5, Canada, [‡]Universite Libre de Bruxelles, 1050 Brussels, Belgium.

The amino terminal segment of the gp32 glycoprotein of SIV has been identified as an important region for membrane fusion. A synthetic dodecapeptide corresponding to this amino terminal segment, SIVwt, can promote the fusion of liposomes. This peptide inserts at an oblique angle into the membrane. If the amino acid sequence, but not composition, of this peptide is changed, the resulting peptide, SIVmutV, no longer promotes fusion and it is oriented perpendicular to the plane of the bilayer. In the present work we demonstrate that SIVwt, but not SIVmutV, can lower the bilayer to hexagonal phase transition temperature of model membranes composed of dipalmitoleoyl phosphatidylethanolamine. In addition the SIVwt promotes the formation of structures which give rise to isotropic ^{31}P NMR signals in mixtures with monomethyldioleoyl phosphatidylethanolamine. These structures are not formed with SIVmutV and their formation with SIVwt is suppressed with lysophosphatidylcholine. These results suggest that the observed correlation between oblique insertion of viral fusion peptides into membranes and their fusogenicity may be a consequence of these peptides increasing negative monolayer curvature.

Th-AM-D4

CERAMIDES IN THE MODULATION OF MEMBRANE FUSION. ((F.M. Goñi, M.B. Ruiz, G. Basáñez, M.P. Veiga and A. Alonso)) Department of Biochemistry, University of the Basque Country, P.O. Box 644, 48080 Bilbao, Spain.

The effect of ceramides on phospholipase C-induced liposome fusion has been explored both by incorporating pure ceramides in the bilayer composition and by *in situ* synthesis, with sphingomyelin (SM) and sphingomyelinase. Phospholipase C readily induces fusion of large unilamellar vesicles composed of PC:PE:CHOL (2:1:1) (Nieva *et al.*, Biochemistry 28, 7364, 1989); instead, no fusion is detected when SM:PE:CHOL (2:1:1) liposomes are treated with sphingomyelinase. Liposomes containing SM:PC:PE:CHOL (1:1:1:1) do not fuse either with phospholipase C or with sphingomyelin, in fact, the enzyme hydrolytic activities are strongly inhibited under these circumstances; however, treating these liposomes with both phospholipase C and sphingomyelinase leads to rapid vesicle fusion. Vesicles containing PC:PE:CHOL (2:1:1) in which 5-10% of the phospholipid has been substituted for ceramide, when treated with phospholipase C, fuse with a shorter lag time than in the absence of ceramide, however this effect is not as clear as that of diacylglycerols (Nieva *et al.*, Biochemistry 32, 1054, 1993). DSC calorimetric studies of the effect of ceramides on phase transitions have been also performed and correlated with the structural effects of ceramides on membrane stability.

Th-AM-D5

STUDY OF FLICKERING AND SECURELY OPEN FUSION PORES BETWEEN CELLS AND PLANAR MEMBRANES. ((G.B. Melikyan, W.D. Niles, V.A. Ratinov*, M. Karhanek, J. Zimmerberg*, F.S. Cohen)) Dept. Physiology, Rush Medical College, Chicago, IL 60612. *LTPB, NICHD, NIH, Bethesda, MD 20892.

The evolution of fusion pores between influenza virus hemagglutinin expressing fibroblasts and planar bilayer membranes was monitored by time-resolved admittance measurements. Typically, pores instantaneously opened (< 1 ms) to conductances of about 2 nS. They then exhibited semistable conductances, 2-20 nS, before either closing (termed flicker) or remaining semistable (termed securely open) before fully enlarging to final conductances on the order of a few μS. The distributions of initial conductances were the same for both types of pores and both continued to grow at about the same rate (ca. 5 nS/s) for a few hundred ms, implying their initial identity. However, securely open pores had longer lifetimes and reached higher conductances than the flickering pores. Securely open pores tended to initiate their final enlargement from the maximal conductance achieved within the semistable stage. In contrast, after the early increases, conductances of flickering pores tended to decrease prior to instantaneous closure. We conjecture that flickering and securely open pores are fundamentally the same throughout their sojourn in the semistable stage. The greater (or smaller) the conductance the more (less) likely a pore will fully open. (Supported by NIH GM 27367).

Th-AM-D6

PROPERTIES OF THE INITIAL FUSION PORES OF THE BACULOVIRUS-INDUCED CELL-CELL FUSION ((I.PLONSKY, and J.ZIMMERBERG,LTPB,NICHD,NIH, BETHESDA,USA))

In order to characterize baculovirus-mediated syncytia formation of SF9 cells, we performed double whole-cell and time-resolved admittance measurements of fusion pore conductance. Double whole-cell recording data shows the difference between the intrinsic gap junctional channels (GJ) and initial fusion pores (FP). GJ have smaller conductances (≈100pS), potential-dependence and flicker. FP have bigger conductances (1.1 nS mean), don't flicker and usually widen with a higher component of low-frequency noise. To chacterize the kinetics of fusion by admittance measurements, fusion was triggered by injecting highly buffered acid solutions from a micropipette placed close to the cell. Waiting time (t_w) values (time intervals between triggering and the appearance of the first fusion pore) were surprisingly small: $0.213<t_w<2.64$ s; median=0.627 s. The distribution of t_w was plotted as the probability that fusion occurred after time t ($P_f>t$). The distribution was optimally fitted by two exponentials with equal rate constants of 0.39 s^{-1} (R^2 =0.93, n=49), which indicates an existence of at least two rate limiting steps from acidification to fusion.

Th-AM-D7

ARCHITECTURE OF THE REGION OF VESICLE-PLANAR MEMBRANE CONTACT PRIOR TO MEMBRANE FUSION. ((W.D. Niles and F.S. Cohen)) Department of Molecular Biophysics and Physiology, Rush Medical College, Chicago, IL 60612.

Membrane fusion between a phospholipid vesicle and a planar lipid bilayer is preceded by an initial adhesion over a region of each membrane. We have used a resonance energy transfer (RET) imaging microscope with calibrated video cameras to determine both the area of the contact region and the distances between the membranes within this zone. Large vesicles (5-20 μm in diameter) are labeled with the donor fluorophore coumarin-phosphatidylethanolamine (PE), while the planar membrane is labeled with the acceptor rhodamine-PE. When vesicles are directed at the planar membrane in the presence of Ca^{2+} without an osmotic gradient, the fraction that becomes stably attached is Ca^{2+}-dependent. With a high sterol-containing lipid composition and solvent-free planar membranes, the dyes do not transfer, allowing the adherent state to be quantitated. Contact regions are detected by the sensitization of rhodamine fluorescence when the directly excited coumarin is nearby. Both the area of the region of contact and the distance between the bilayers in this zone are highly variable, indicating undulation of the membranes. The undulation is characterized by the 2-D spatial correlation function. This distribution of distances within the contact region varies with Ca^{2+} in a complex manner. Increased [Ca^{2+}] produces decreased intermembrane separation within the region of contact. Supported by NIH GM27367.

Th-AM-D8

PROTEIN-INDUCED ADHESION AND FUSION OF LIPOSOMES ((K. Arnold, O. Zschoernig, G. Koehler))
Institute of Medical Physics and Biophysics, University of Leipzig, FRG

It has been shown that water-soluble proteins are capable of inducing fusion of acidic phospholipid vesicles. The increase of the membrane surface hydrophobicity is one of the important factors contributing to strong adhesion and fusion of liposomes. The correlation of protein binding, surface adhesion and fusion of liposomes was studied for lysozyme, polylysine and annexin V. Fusion was monitored by a fluorescence probe mixing assay and intermixing of vesicle contents. Decreases of the surface dielectric constant were detected by the shift of the fluorescence signal of dansyl-PE. The creation of hydrophobic patches at the bilayer surface was studied by the fluorescence of bis-ANS. The protein binding was determined from electrophoretic measurements of the zeta potential and resonance energy transfer from protein tryptophan to fluorescence probes located in the bilayer. Lysozyme, poly(L-lysine) and annexin V are able to fuse acidic liposomes at low pH. Under these conditions a decrease of the surface dielectric constant and an increase of the fluorescence of bis-ANS are observed. These findings indicate an increase of the surface hydrophobicity accompanied by a strong adhesion of liposomes. Electrophoretic measurements show the importance of electrostatic interactions for the protein adsorption. It could be shown for lysozyme that the adsorption is followed by a partial penetration of the protein into the bilayer. Hydrophobic segments are exposed to water. The insertion of protein segments into the bilayer may result in the local destabilization necessary for fusion to occur. This research was supported by the Deutsche Forschungsgemeinschaft (SFB 197).

Th-AM-E1

PROTEIN RELAXATION AND HEME-IRON DISPLACEMENT ((E.E. Di Iorio, I. Tavernelli and W. Yu)) ETH, Zurich, Switzerland.

The crystal structure at 1.4 Å resolution of CTT-Hb-III, a monomeric hemoglobin extracted from the larvae of the insect *Chironomus thummi-thummi*, shows a myoglobin-like folding and a nearly planar heme in both deoxy and CO derivatives (1). This contrasts with all reports on other hemoglobins and myoglobins, where only the ligated derivatives display a planar heme. The increase of the geminate ligand binding enthalpy, observed in flash photolysis measurements on Mb above ~160 K, is generally attributed to a larger heme-iron displacement in the high compared to the low temperature photoproduct, brought about by protein relaxation. According to this interpretation, geminate ligand recombination to CTT-Hb-III should not display any significant increase of its activation barrier upon relaxation.

CO binding kinetics to CTT-Hb-III between 40 K and 300 K show that geminate ligand recombination is well described by a single enthalpy distributed process, whose peak position increases by ~8.5 kJ/mol between 160 and 300 K, compared to ~10 kJ/mol reported for SW-Mb (2). Unless the X-ray data on CTT-Hb-III are proven to be wrong, this shows that the iron displacement is not the only structural element that determines the change in ligand binding activation barrier upon protein relaxation. Furthermore, relaxation in CTT-Hb-III produces also a narrowing of the enthalpy distribution such that at ~290 K geminate CO binding becomes exponential in time. Finally, Hpeak depends on temperature also below 160 K, with a first transition which can be estimated to be centred at ~50 K, followed by a small drift in the temperature region between ~100 K and ~160 K.

1) Steigeman & Weber (1979) J. Mol. Biol. 127, 309-338
2) Steinbach et al. (1991) Biochemistry 30, 3988-4001.

Th-AM-E2

HEME COORDINATION STATES IN NITRIC OXIDE COMPLEXES OF MYOGLOBIN PROXIMAL LIGAND MUTANTS ((S.M. Decatur, G.D. DePillis, and S.G. Boxer)) Department of Chemistry, Stanford University, Stanford, CA 94305-5080.

When nitric oxide (NO) binds to ferrous heme proteins, it is capable of forming both five-coordinate and six-coordinate complexes; this contrasts sharply with the behavior of ligands such as CO and O_2, which form only six-coordinate ferrous heme protein complexes. For example, wild type myoglobins form a six-coordinate NO complex at pH 7; however, when the proximal ligand in myoglobin is replaced by a cysteine (H93C) or a glycine plus an exogenous imidazole (H93G(Im)), these mutant myoglobins form NO complexes where the bond between the proximal ligand and the iron is weakened or broken, leaving a five-coordinate NO-heme. Little is known about the specific structural or environmental determinants of coordination state in these proteins. In the sperm whale myoglobin mutant H93G, the proximal ligand to the iron can be varied systematically with respect to its size, shape, and chemical properties.[1] In this report, we present spectroscopic data on myoglobin-NO complexes where the properties of the proximal ligand have been altered in order to explore the determinants of heme coordination state.

[1] DePillis, G.D., Decatur, S.M., Barrick, D., and Boxer, S.G. (1994) *J. Am. Chem. Soc. 116*, 6981-6982.

Th-AM-E3

CHARACTERIZATION OF HEME AND PROXIMAL LIGAND OUT-OF-PLANE VIBRATIONAL MODES IN PROXIMAL CAVITY MUTANTS OF MYOGLOBIN

((Stefan Franzen[1], Sean M. Decatur[3], Gia DePillis[3], Steven G. Boxer[2], R. Brian Dyer[1], William H. Woodruff[1]))
1. Biosciences and Biotechnology Group, CST-4 MS C345, Los Alamos Natl. Laboratory Los Alamos, NM 87545 2. Dept. of Chemistry, Stanford University, Stanford, CA 94305

The correlation between vibrational spectroscopy and structure of the active site in Mb is investigated using mutants in which the proximal histidine has been replaced by glycine, H93G [1] leaving a cavity which can be filled by exogenous ligands to iron [2]. Resonance Raman (RR) spectroscopy of the heme is compared to structural data on metaquo Mb obtained from X-ray crystallography [1] and NMR [3]. Substituted imidazoles (Im) and pyridines (Pyr) allow isotope effects (d3-Im, d5-Pyr), conformational effects (2- and 4-Methyl Im and Pyr), and electronic effects (4-Br Im and fluoro Pyr) to be probed. Double mutants allow cavities without hydrogen bonding to Im (S92A/H93G), and altered rotation angles of the Im ring (S92T/H93G). The goal is to assign functionally relevant heme vibrational modes (e.g. the 220 cm^{-1} mode thought to be a Fe-L stretch and used extensively to probe the proximal geometry in deoxy Mb and hemoglobin) to serve as a structural basis for time-resolved spectra. For example, the RR spectrum of deoxy H93G(Im) shown in the Figure (--) has a larger intensity, shifted frequency, and decreased asymmetry of the Fe-L out-of-plane mode compared to wild type Mb (—). In H93G(4-MeIm), the 4-Me group has a similar position to the $-CH_2-$ in native histidine in contact with the F-helix. The steric forces of 4-MeIm in the cavity result in a RR spectrum similar to wild type (⁻).

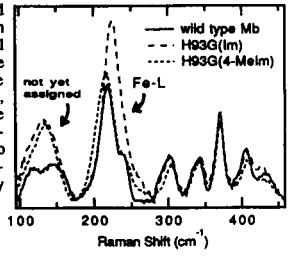

1. Barrick, D. Biochem. (1994) 33: 6546
2. DePillis et al. JACS (1994) 116: 6981
3. Decatur and Boxer Biochem. in Press

Th-AM-E4

MODELING THE CROSS-LINKING OF HUMAN HEMOGLOBIN

((S.L. Chan†, I.D. MacDonald‡, J. Rydall‡, C. Lim†, D. Pliura‡))
† Dept. of Molecular & Medical Genetics, 1 King's College Circle, University of Toronto, M5S 1A8, Canada ; ‡ Hemosol Inc., 115 Skyway Ave., Etobicoke, Ontario, M9W 4Z4, Canada. (Spon. by D.O. Tinker)

The cross-linking of hemoglobin is important towards developing a blood substitute. Cross-linking is usually achieved via reagents that react selectively with amine groups on lysine side-chains and the N-termini of hemoglobin. In particular, o-raffinose selectively attack the Lys 82 and the N-terminal valine on the β side-chains of human hemoglobin. Since the reaction mechanism involves a nucleophilic attack by a lone pair on the amine nitrogen, deprotonation of the amine group is essential to the reaction. Electrostatic calculations on human deoxy-hemoglobin confirmed that Lys 82 and the N-terminal valine on the β side-chain have the highest electric potential among the amine groups and hence are most likely to be deprotonated. The experimentally observed selectivity can thus be rationalized.

This work is supported by the Protein Engineering Network of Centres of Excellence of Canada.

Th-AM-E5

MECHANISM FOR THE DISPLACEMENT OF BOUND OXYGEN FROM HEMOGLOBIN AS A SUPEROXIDE RADICAL ((C. Balagopalakrishna, O. Abugo, J.M. Rifkind)) NIA, NIH, Gerontology Research Center, Baltimore, MD 21224

Autoxidation of hemoglobin can proceeed via an outersphere reaction with oxygen or an innersphere electron transfer process involving the displacement of oxygen already bound to the heme. Recent evidence indicates that with partially oxygenated hemoglobin the dominant reaction involves the bound oxygen. The mechanism for this oxidation process has been studied by low temperature EPR. We have been able to follow changes in the iron producing an increase in methemoglobin. The initial growth of bis-histidine complex B known to be associated with a nearby oxygen atom is suggestive of a displacement of the bound oxygen by the distal histidine. We have also been able to detect the formation of an anisotropic free radical signal. Oxygen-17 substitution confirms that this free radical signal corresponds to superoxide. The ability to detect a stable signal is attributed to superoxide trapped within the heme pocket and therefore unable to dismutate. We have used variation in pH to show how the autoxidation reaction is modulated by heme pocket dynamics. Lowering the pH below 7 enhances autoxidation. In the low temperature EPR studies lower pH increases the rate for forming the superoxide but also increases the rate for the superoxide to escape from the pocket and dismutate. These studies link the autoxidation to ligand pocket mobility required for the nucleophilic displacement of bound oxygen as a superoxide.

Th-AM-E6

COMMUNICATION OF EFFECTOR BINDING DOMAINS WITHIN THE CENTRAL CAVITY OF COHbA AT LOW pH. ((RE Hirsch, DS Gottfried, I Lalezari, P Lalezari, AS Acharya, and JM Friedman)). Albert Einstein College of Medicine and Montefiore Medical Center, Bronx, NY.

It is well established that the oxygen affinity of hemoglobin (Hb) is decreased by organic phosphates (DPG, IHP) and synthetic allosteric effectors binding to the Hb central cavity. Functional studies show synergistic activity when both are present. A fluorescent analog of DPG, 8-hydroxy-1,3,6-pyrenetrisulfonate (HPT) is used to monitor the interaction of these effectors at neutral and slightly acidic pHs. Binding of HPT to stripped deoxy Hb (pH 7.35) results in a substantial decrease in the Hb intrinsic fluorescence intensity (as well as HPT emission) whereas the addition of HPT to oxy HbA results in little or no fluorescence change. The deoxy change is reversible upon Hb oxygenation. These results are as expected since it is known that HPT binds with much higher affinity to deoxy than to oxy hemoglobin. The addition of HPT to COHbA at pH 6.35 causes the intrinsic fluorescence of Hb to decrease 31% compared to 7.9% for COHbA at pH 8.0 consistent with IHP binding studies. The fluorescence changes are reversed upon addition of IHP or L35 (a clofibric acid derivative) in a differential manner indicating that IHP and L35 displace HPT. Changes in the Hb and HPT fluorescent lifetimes correlate with the steady state changes. While the reversal is expected for IHP (since it binds to the DPG site with greater affinity than HPT), the displacement of HPT by L35 is surprising since L35 binds at a site 20Å deeper into the central cavity compared to DPG. The results clearly demonstrate that L35 displaces HPT. Given the spatially distinct binding sites of L35 and DPG, long range communication in the central cavity between these two independent regions is implied.

Th-AM-E7

CONTRIBUTIONS OF SOME HISTIDYL RESIDUES TO THE BOHR EFFECT OF HB A ((D. P. Sun, M. Zou, N. T. Ho, V. Simplaceanu, T.-J. Shen, H.-W. Kim, and C. Ho)) Department of Biological Sciences, Carnegie Mellon University, Pittsburgh, PA 15213

In this work, we assess the contributions from the surface histidyl residues in the α-chain of Hb A, as well as the histidyl residue in the β-chain at position 143 (β143), near the carboxyl terminus. Previously, investigators in our laboratory have monitored the variation of aromatic proton resonances, arising from the C-2 and C-4 protons of histidyl residues of Hb A, as a function of pH and buffer conditions. By applying site-directed mutagenesis to an *Escherichia coli* Hb expression plasmid (pHE2), we have constructed six recombinant mutant Hbs, in each of which a single histidyl residue is replaced by a glutaminyl residue. The mutated histidyl residues are α20His, α50His, α72His, α89His, α112His, and β143His. In principle, by comparing the ^{1}H-NMR spectra of Hb A in the CO and deoxy forms with those of the recombinant mutant Hbs, we can identify the aromatic resonances arising from the C-2 and C-4 protons of these histidyl residues in HbCO A and deoxy-Hb A. From the change of the pK values of the histidyl residues upon oxygenation , we can calculate the contributions of individual histidyl residues to the total Bohr effect of Hb A. Our results have shown a possible degeneracy of the assignment of α20His and α112His, indicating important interaction between these two residues. The relationship of the present results to the molecular basis of Bohr effect will be discussed. [supported by a grant from NIH (HL-24525)].

Th-AM-E8

MODELING THE ALLOSTERIC TRANSITION IN HEMOGLOBIN: STRUCTURE OF VARIOUS LIGATION STATES OF CYANOMETHEMOGLOBIN. ((V. Jayaraman*, G. K. Ackers† and T. G. Spiro*)) *Dept. of Chemistry, Princeton University, Princeton, NJ 08544 and †Dept. Biochem. and Mol. Biophysics, Washington Univ. School of Medicine, St. Louis, MO 63110.

Direct analysis of the properties of the various ligation states in Hemoglobin (Hb) has been precluded due to (a) extreme lability and rapid exchange of the ligand between the subunits, (b) dissociation of the tetramers into dimers and reassociation to form tetramers with different arrangements of ligated sites. The first problem has been overcome by using valency hybrids where Fe^{2+} of the heme is oxidized to Fe^{3+} (met) and CN^- is used as the ligand. To circumvent the second problem studies have been performed on mixtures of these intermediates and their parents. The UV resonance Raman spectra clearly indicate that the quaternary transition from the R to the T state has at least two intermediates. The T state on gaining two ligands on the same dimer switches to a T' state. The H-bonds present in the $\alpha_1\beta_2$ interface appear to be weaker in this state relative to the T state. The second intermediate structure is observed predominantly in the triply ligated state which is associated with an R quaternary structure having tertiary changes near the heme which is deligated. This structure appears to be less stable than the R state and hence exhibits a greater affinity towards ligation which is known as quaternary enhancement. Thus, it appears that while the two state MWC model has been useful in understanding cooperativity, in hemoglobin there are at least three states present and the various ligation states can be represented as an equilibrium mixture having two or more of these states.

Th-AM-E9 (Abstract from Th-AM-B3 presented here)

PORIN AND VDAC

Th-AM-SymII-1

SOLUTE SPECIFICITY OF PORIN CHANNELS. ((J. ROSENBUSCH)) Univ. of Basel.

Th-AM-SymII-2

MOLECULAR DESIGN OF THE MITOCHONDRIAL PORIN, VDAC. ((C.A. Mannella)) The Wadsworth Center, Empire State Plaza, Box 509, Albany, NY 12201-0509

Considerable information about the structure of the voltage-gated channel in the mitochondrial outer membrane has come from electron microscopic studies of crystalline arrays of the channel induced in the membranes by phospholipase A_2 and embedded in vitreous ice or aurothioglucose. Compared with bacterial porins, the pores in the VDAC arrays are wider and are not related by local 3-fold symmetry. Studies of different crystal polymorphs have defined two "open" states of the VDAC channel, which differ primarily in the position of a flexible arm. Immunolabelling experiments indicate that this arm is composed (at least in part) of the N-terminal segment of the polypeptide, and is exposed at the surface of the outer membrane facing the inner membrane. Circular dichroism (CD) studies of a synthetic N-terminal peptide suggest that it can form an amphipathic α-helix. CD spectra of purified VDAC are very similar to those of bacterial porins, suggesting that VDAC may fold as a β-barrel. Correlative CD and liposome-swelling studies at different pH and temperature have defined three states of VDAC, "open" (~60% β-sheet content), fully but reversibly "closed" (~30% β), and irreversibly deactivated (no β). (Supported by NSF grant MCB9219353.)

Th-AM-SymII-3

PhoE PORIN OF E. COLI: STRUCTURE AND FUNCTION. ((J. TOMMASSEN)) State Univ. of Utrecht.

Th-AM-SymII-4

THE STRUCTURAL CHANGE RESPONSIBLE FOR VOLTAGE GATING IN VDAC ((M. Colombini* and M. Forte#)) *Dept. Zoology, U. Maryland, College Park, MD 20742, #Vollum Inst., Oregon Hlth. Sci. Univ., Portland, OR 97201.

When reconstituted into phospholipid membranes, the mitochondrial channel, VDAC, forms large aqueous pores approximately 3 nm in diameter. Using site-directed mutations, we have mapped the wall of the channel and concluded that it is a barrel formed by 1 α helix and 12 β strands. Each channel has two gating processes that result in channel closure whether positive or negative potentials are applied. These closed states can be studied because while highly resistive to the flow of organic anions, they are still permeable to simple salts. Thus the closed conformation differs from the open in that portions of the wall of the channel seem to be forced out of the membrane, resulting in a reduced pore diameter and volume. The regions that move have a net positive charge and account for both the charge motion essential for voltage gating and the dramatic change in selectivity. This motion establishes the electrostatic barrier responsible for the reduction in permeability of the mitochondrial outer membrane to important anionic metabolites (e.g. ATP, ADP, succinate, citrate). This closing mechanism explains the fast rate (μsec to msec) of channel opening and the slow, voltage-dependent rate of channel closure (msec to sec). In addition, rapid opening may be favored by a protein strand in the sensor region where mechanical stress may develop due the constrained motion. Thus the current working mechanism for voltage gating in VDAC is highly constrained by experimental measurements and accounts for the known properties of the channel. (Supp. by ONR grant N00014-90-J-1024 and NIH grant GM 35759)

Th-AM-F1

7-Å RESOLUTION PROJECTION STRUCTURE OF THE ERYTHROCYTE CHIP28 WATER CHANNEL BY CRYO-ELECTRON MICROSCOPY. ((A. K. Mitra*, A. N. van Hoek#, M. C. Wiener#, A. S. Verkman#, and M. Yeager*)) *The Scripps Research Institute, Dept. of Cell Biology, La Jolla, CA 92037. #University of California San Francisco, Cardiovascular Research Institute, Department of Biochemistry and Biophysics, San Francisco, CA 94143.

Osmotic water transport across plasma membranes in erythrocytes and several epithelial cell types is facilitated by the integral membrane protein CHIP28, a water-selective channel. In order to determine the structure of CHIP28 in the membrane, large (1.5-2.5μm diameter), highly ordered, 2-dimensional (2-D) crystals of purified and deglycosylated erythrocyte CHIP28 were generated by *in vitro* lipid reconstitution. A 12-Å resolution projection density map of CHIP28 derived from negatively-stained 2-D crystals revealed the molecular contacts, tetrameric organization and packing of oblong-shaped (37x25Å) CHIP28 monomers in a tetragonal unit cell (a=b=99.2Å) [Mitra *et al., Biochemistry* in press (1994)]. Since the 2-D crystals display order (~12Å) beyond the typical limit achieved by negative staining (15-20Å) they are amenable to higher-resolution analysis by cryo-electron microscopy. We have now recorded minimal-dose images and electron diffraction patterns from unstained CHIP28 2-D crystals preserved in the frozen-hydrated state at -172° C. The electron diffraction patterns display reflections to ~4-Å resolution. Computed transforms of images display order to ~8-Å resolution before and to ~5-Å resolution after correcting for lattice distortions. A preliminary projection density map at a nominal resolution of 7Å indicates that each monomer is composed of two domains and reveals finer details of the molecular envelope and monomer interactions within the tetramer. The map also displays densities characteristic of α-helices in each monomer.

Th-AM-F2

THE WATER PERMEABILITY PER MOLECULE OF MIP IS LESS THAN THAT OF CHIP. ((Grischa Chandy, Mike Kreman*, Deborah L. Laidlaw, Guido A. Zampighi*, James E. Hall)) Dept. of Physiology and Biophysics, UC Irvine, Irvine, CA 92717-4560 and *Dept. of Anatomy, UCLA, Los Angeles, CA 90049

Our overall goal is to understand the physiological role of MIP. Since MIP's closest relative, water channel collecting duct (Aquaporin-2), is a water channel, we investigated MIP's ability to flux water. Oocytes injected with 100 ng of MIP cRNA swell 3-4 fold faster than control (water-injected oocytes), whereas oocytes injected with 50 ng of CHIP (Aquaporin-1) cRNA swell about 20 fold faster than control oocytes. MIP thus appears to be much poorer at enhancing water permeation than CHIP. This low apparent permeability could be an intrinsic property of MIP or a result of low expression or insertion into the plasma membrane. Western blots using a C-terminal antibody to MIP show oocytes injected with MIP cRNA produce a significant amount of a 26 kD protein. This result rules out low expression but not low insertion as a cause of the apparent low MIP-induced water permeability. To eliminate low insertion we used a novel oocyte freeze-fracture technique to quantify the density of heterologously expressed protein in the oocyte plasma membrane. We estimatedthe number of CHIP particles in the oolemma at 650 ± 50 particles/μm^2 (50 ng cRNA) and the number of MIP particles at over 4000 particles/μm^2 (100 ng cRNA). These data indicate that CHIP monomers have a permeability of 7.7 x 10^{-14} cm^3/s and MIP monomers have a permeability of less than 7.5 x 10^{-16} cm^3/s at 23°C. Thus CHIP facilitates water transport more than 100 times more effectively per monomer than MIP. cRNAs were transcribed using modified Bluescript plasmids containing coding sequences flanked by β-globin 5' and 3' untranslated regions (Kind gifts from Dr. Peter Agre). Supported by NIH grants EY 05661 to JEH and EY 04110 to GAZ.

Th-AM-F3

EFFECT OF HYPOTONICITY AND SODIUM TRANSPORT RATE ON CELL VOLUME OF A6 EPITHELIA. ((W. Van Driessche, J. Simaels and P. De Smet)) Laboratory for Physiology, K. U. Leuven, 3000 Leuven, Belgium. (Spon. by J. B. Parys)

Cell thickness (T_c), short-circuit current (I_{sc}) and transepithelial conductance (G_t) of distal kidney epithelia (A6) perfused with NaCl solutions were recorded. In control conditions T_c decreased slowly at a rate of 9.3 % per hour. A negligible water permeability of the apical barrier was demonstrated by the lack of a volume change following a reduction of the apical osmolality from 260 to 140 mOsm/kg. The inhibition of Na^+ uptake did not affect cell volume in isotonic conditions. Blocking active transport with ouabain for 60 min increased T_c by 12.1 % above the control baseline. The activation of Na^+ transport with insulin or oxytocin did not alter cell volume significantly. Basolateral Ba^{2+} (5 mM) elicited a significant increase in T_c of 16.3 % above control, whereas quinine, did not change T_c significantly. Basolateral hypotonicity elicited a rapid rise in T_c followed by a regulatory volume decrease (RVD). An RVD was still recorded after altering apical Na^+ uptake. Inhibition of active transport with ouabain as well as blocking basolateral K^+ efflux with Ba^{2+} or quinine abolished the RVD. The effect of ouabain seems to be caused by a cellular K^+ depletion whereas Ba^{2+} and quinine most likely act by blocking K^+ excretion.

Th-AM-F4

CLONING AND FUNCTIONAL EXPRESSION OF A GASTRIC PKA- AND VOLTAGE-ACTIVATED Cl^- CHANNEL THAT IS STABLE AT ACID pH. ((D. H. Malinowska, E. Y. Kupert and A. M. Sherry)) Dept. of Mol & Cell Physiol, Univ. of Cinc Coll of Med, Cincinnati, OH 45267-0576.

The gastric Cl^- channel which is thought to be essential for HCl secretion is PKA-, voltage- and acid-activated (AJP 264: C1609-C1618, 1993). cDNA encoding a Cl^- channel was isolated from an unamplified rabbit gastric library, sequenced and expressed in *Xenopus laevis* oocytes. The predicted protein (ClC-2G, 898 amino acids, M_r 98,433 Da) had 93% overall similarity to ClC-2 and contained 12 potential transmembrane domains (D1-D12). However, in the cytosolic loop following D12, homology with ClC-2 decreased to 74% and 6 amino acids were deleted. In this region, amino acid changes (H to S_{650} and L to S_{749}) introduced two new potential PKA phosphorylation sites ($RRQS_{650}$ and RKS_{749}) not present in ClC-2. cRNA-injected oocytes expressed a Cl^- channel with characteristics indistinguishable from those of the native gastric channel and different from ClC-2. Thus ClC-2G was active at acid pH, had a linear I-V curve, a slope conductance of 29±1 pS at 800 mM CsCl, a reversal potential of +30±3 mV under a 5-fold Cl^- gradient and an anion selectivity of $I^- > Cl^- > NO_3^-$. In contrast to ClC-2, ClC-2G was activated *in vitro* with PKA catalytic subunit plus ATP, as was the native gastric Cl^- channel. ClC-2G's structural and functional properties suggest that it may be encoded by an alternatively spliced transcript of the ClC-2 gene and that it is the Cl^- channel essential for HCl secretion. Supported by DK43816, DK43377 (DHM) and a Ryan Fellowship (AMS).

K^+ CHANNELS II

Th-AM-G1

THE INWARD RECTIFIER POTASSIUM CHANNEL FROM HUMAN HEART AND BRAIN: CLONING AND STABLE EXPRESSION IN A HUMAN CELL LINE. ((M. D. Ashen, B. O'Rourke, K. A. Kluge, D.C. Johns, G. F. Tomaselli)) Division of Cardiology, Department of Medicine, The Johns Hopkins School of Medicine, Baltimore, MD 21205.

We have cloned the human homolog of the inward rectifier potassium channel from both heart and brain tissue (HHBIRK1). The human clones were identical to each other in their coding regions and highly homologous to the mouse macrophage (IRK1) channel. Northern blot analysis revealed the expression of HHBIRK1 mRNA in various human tissues including heart, brain, skeletal muscle, placenta and lung. The inward rectifier currents from human and mouse clones were characterized using a novel strategy for episomal stable ion channel expression in a human cell line. The permeability of the expressed inwardly rectifying channels was greater for K^+ than Rb^+ while no current was observed when K^+ was replaced by Na^+. A prominent time and voltage-dependent block was observed in the presence of Ba^{2+} while a small decay in the steady state current was observed with millimolar concentrations of Na^+. Single channel conductances of 49.1 ± 3.3 pS (n=6) and 40.2 ± 2.5 pS (n=3) (p = 0 .005) were obtained for the HHBIRK1 and IRK1 clones, respectively. These results indicate that sequence dissimilarities between human and mouse inward rectifier potassium channels may have significant functional consequences .

Th-AM-G2

Cloning and Functional Expression of Human Pancreatic and Brain ATP-sensitive Potassium Channels. ((Kim W. Chan, Jinliang Sui, John A. A. Ladias* and Diomedes E. Logothetis)) Mount Sinai School of Medicine,CUNY, New York, NY. and *New England Deaconess Hospital, Harvard Medical School, Boston, MA.

Using probes spanning the M1 through the M2 region of a cloned G-protein-gated K channel (Kubo *et al.*, 1993; Dascal *et al.*, 1993) we screened a human brain cDNA library. A weakly hybridizing clone revealed a unique sequence that showed 65% similarity to the G-protein-gated K channel. Northern blot analysis showed abundant message corresponding to our brain clone in human pancreas. Screening a human pancreatic cDNA library yielded several strongly hybridizing clones. One of these positive clones was fully sequenced and functionally expressed in *Xenopus* oocytes and mammalian cells. In *Xenopus* oocytes, expression of this channel yielded microampere levels of a potassium conductance sensitive to 200 μM $BaCl_2$. In CHO mammalian cells, expression of this channel showed weak inward rectifying properties with a conductance of 53 pS under symmetrical potassium solutions and intraburst kinetics similar to the native pancreatic K_{ATP} channel. The cardiac ATP-sensitive channel K channel was recently reported from rat and human sources (rcK_{ATP}, hcK_{ATP}, Ashford *et al.*, 1994). Functional characterization of the rat channel (rcK_{ATP}) showed a 70 pS bursting channel with kinetic properties and pharmacological sensitivities similar to cardiac K_{ATP} channels. Both our human brain and pancreatic channels (hbK_{ATP}, hpK_{ATP1}) showed almost identical amino acid sequences to the hcK_{ATP} channel which shows differences from rcK_{ATP} in 28 amino acid positions. A second strongly hybridizing pancreatic clone showing unique sequence accounted for one of the messages on the Northern blot suggesting that it represents a unique isoform (hpK_{ATP2}).

Th-AM-G3

HSP70 INTERACTS WITH THE KV1.3 K+ CHANNEL PROTEIN DURING BIOSYNTHESIS. ((Michael Strong, K.G. Chandy and G.A. Gutman)). Depts. of Phys. & Biophys. and Micro. & Mol. Gen., UC Irvine, Irvine, CA 92717-4560.

We are using a vaccinia virus expression system to purify and study the structure of the Kv1.3 protein. This system can be used to study the biochemical modifications leading to maturation of the protein, as well as the mechanisms which regulate biosynthesis, transport to the surface and turnover. Kv1.3 is synthesized as three forms which run at 59, 60, and 65-75kD on SDS-PAGE gels, and heterogeneous N-linked glycosylation is responsible for much of the difference between these forms. Densitometric scans of data from pulse-chase experiments (10' labeling) show that over 50% of the labeled population of Kv1.3 protein is lost within 2 hours of synthesis. This short time-course of degradation might indicate an ER degradative mechanism in which members of the chaperonin family and metalloproteases degrade misfolded or misassembled proteins. To test whether Kv1.3 associates with chaperonins during biosynthesis, we performed experiments using the VV system and mAb to hsp70. A 59kD band is immunoprecipitated (IP) with hsp70 Ab in dually-infected cells that is not present in either of three negative controls, namely uninfected cells, T7 virus cells or Kv1.3 virus cells. This band runs similarly to the 59kD band seen upon IP with Kv1.3 Ab. To show that this co-immunoprecipitated band is indeed Kv1.3, we performed an IP with hsp70 Ab followed by an immunoblot with Kv1.3 Ab. The immunoblot shows detection of the 59 and 60kD forms as co-immunoprecipitated with hsp70. These results suggest that the cytosolic chaperone hsp70 participates in the biosynthesis of Kv1.3 perhaps by helping to mediate folding and polypeptide transfer into the ER.

Th-AM-G4

SINGLE CHANNEL CHARACTERISTICS OF A G-PROTEIN LINKED EPITOPE-TAGGED K+ CHANNEL (GIRK1-cp) EXPRESSED IN STABLY TRANSFECTED MAMMALIAN CELLS. ((J. Murphy*, A. Kuznetsov#, L.H. Philipson#, G. Szabo*)) *U. Of Virginia, Charlottesville, VA 22908 and #U. Of Chicago, Chicago IL 60637.

We have investigated the biophysical characteristics and regulatory mechanisms of a stably expressed, epitope-tagged inwardly rectifying K^+ channel GIRK1-cp, using the excised patch mode of the patch clamp technique. In cardiac myocytes, a corresponding molecule (GIRK1) is believed to generate I_{KACh}, the inwardly rectifying potassium channel coupled to muscarinic receptors via the G protein G_K. GIRK1, recently cloned from a rat insulinoma cDNA library, was epitope-tagged at the C-terminal end with the C peptide of human pro insulin and transfected into two mammalian cell lines, human embryonic kidney (HEK293) and mouse insulinoma (BTC3) cells. While both cell lines expressed GIRK1-cp, we found no evidence of G protein dependent channel activity in transfected HEK293 cells (36 patches, varying conditions). In contrast, application of GTPγS, a trinucleotide that persistently activates G proteins, induced significant inwardly rectifying K^+ channel activity in transfected BTC3 cells (7 out of 50 patches). This channel activity was not seen in untransfected cells (0 out of 22 patches). The slope conductance of the GIRK1-cp-dependent, I_{KACh}-like channel was 39.5 pS ± 1.6 (s.e.m., n=6) while the single channel lifetime was 3.1 ms ± 0.25 (s.e.m., n=6). Channel activity was also observed in the cell attached mode with 50 μM norepinephrine in the pipette. We conclude that while this epitope-tagged inwardly rectifying, G-protein linked K^+ channel is expressed in both cell types, it is functional only in BTC3 cells, where its characteristics are essentially identical to that of I_{KACh}.

Th-AM-G5

PROPERTIES OF A G-PROTEIN LINKED EPITOPE-TAGGED K+ CHANNEL (GIRK1) EXPRESSED IN STABLE TRANSFECTED MAMMALIAN CELLS. ((P. Toth, A. Kuznetsov, G.H. Ma, R.J. Miller, and L.H. Philipson)) Univ. of Chicago, Chicago, IL 60637

We have expressed an epitope-tagged inwardly rectifying G-protein linked K^+ channel, termed GIRK1-cp, at high levels by stable and transient transfection of human embryonic kidney cells (HEK293) and mouse insulinoma cells (BTC3). GIRK1-cp transfected cells expressed a series of polypeptides detected with an antiepitope antibody, the most predominant bands having molecular masses of 59, 62, 68 and 70 kDa. The 59 kDa band corresponds to the predicted mass for the GIRK1 polypeptide plus the 31 amino acid epitope tag derived from the c-peptide of human proinsulin. The higher molecular mass bands are seen to greater extent in the HEK cells than in the insulinoma cells. Immunohistochemical studies show intense staining of both transfected cell types, and both show large immuno-positive intracellular inclusion bodies. Although HEK293 cells expressing GIRK1-cp protein did not show any K^+ currents, fully functional message was present. PolyA^+ RNA prepared from these cells and co-injected into *Xenopus* oocytes with κ opioid receptor cRNA produced inwardly rectifying currents when activated by κ opioid receptor agonists, and were indistinguishable from currents produced by native GIRK1 or GIRK1-cp cRNA prepared *in vitro*. In contrast, transfected BTC3 cells expressing GIRK1-cp expressed currents that were consistent with GIRK1 channels. Whole cell recordings showed pertussis-toxin sensitive currents that were activated by norepinephrine, via the α_2 adrenergic receptor, and galanin, but not somatostatin or adenosine receptor agonists. There is thus a striking difference in functional channel expression in the fibroblastic versus neuroendocrine cell. Expression of functional G-protein coupled K^+ currents demonstrates the utility of this system for further biochemical, cell biological, and biophysical analyses of G-protein-K^+ channel interactions in mammalian cells.

Th-AM-G6

DETERGENT SOLUBILIZATION AND IMMUNOAFFINITY CHROMATOGRAPHY OF K+ CHANNELS FROM STABLY TRANSFECTED MAMMALIAN CELLS

((Mark Yeager, Thomas D. Hong,*, Andrey Kuznetsov#, and Louis H. Philipson#))*
*The Scripps Research Institute, Department of Cell Biology, La Jolla, CA 92037.
#The University of Chicago, Department of Medicine, Chicago, IL 60637.

A major goal of ion channel biochemistry is the purification of channel proteins to facilitate structural studies, and eventually 2-D and 3-D crystallization. To this end, we have explored the solubility characteristics and initial steps in the purification of the human Kv1.5 Shaker-family delayed rectifying K^+ channel. The purification strategy uses the C-terminal peptide of human proinsulin, to which monoclonal and polyclonal anti-peptide antibodies are available. We previously described the construction and characteristics of a C-terminal, epitope-tagged hKv1.5 Shaker-like delayed rectifier expressed in *Xenopus* oocytes and in a stable CHO cell line. We have recently constructed stable cell lines expressing a similarly tagged and functional GIRK1 inwardly rectifying channel. The solubilization of the two proteins from crude membranes was tested at pH 7.5-8.0 for several detergents: octyl-β-D-glucopyranoside, n-decyl-β-D-maltopyranoside, dodecyl-β-D-maltoside, Triton X-100, octylpolyoxyethylene and deoxycholate. For both Kv1.5 and GIRK1, solubilization was achieved using dodecyl-β-D-maltoside and deoxycholate. Antibodies were affinity purified against C-peptide, bound to protein G attached to sepharose beads, and then cross-linked to protein G via dimethyl pimelimidate. The detergent-solubilized suspension was applied to the column, and the protein was eluted by diethylamine buffer and immediately neutralized. Western immunoblots employed the same C-peptide antibodies. Two proteins were detected that represent the glycosylated and non-glycosyated products of Kv1.5. We conclude that the epitope tag method is a feasible approach to purify K^+ channels that will facilitate structural studies. [Support: American Heart Association National Center Grant-in-Aid, the Gustavus and Louise Pfeiffer Research Foundation and NIH RO1HL48908 (MY).]

Th-AM-G7

MOLECULAR RECOGNITION SEQUENCES ENCODED IN THE A SUBDOMAIN OF THE SHAKER T1 DOMAIN. ((N.V. Shen and P.J. Pfaffinger)) Div. of Neuroscience, Baylor College of Medicine, Houston, TX 77030.

Recently, we have shown that wild type Shaker AKv1.1a and Shaw AKv3.1a T1 domains do not heteromultimerize yet contain 3 homologous subdomains (A, B, and C). Therefore, the T1 domain contains molecular recognition sequences important for subfamily specific assembly. To examine the molecular basis for subfamily specificity, chimeras of the Shaker T1 domain (1ABC) were made by substitution with a single homologous Shaw (3ABC) subdomain. These chimeras show that a Shaker type A and B subdomain, but not a C subdomain, are required for heteromultimerization with the wild type Shaker T1 domain. We then focused on the molecular recognition properties of the A subdomain. First, for the 3A1BC chimera, we replaced the Shaw AA11-40 with the 30 homologous amino acids from the 1A subdomain (AA 67-97). This chimera, 31A1BC, is able to heteromultimerize with the wild type Shaker T1 domain. We further analyzed the role of these 30 amino acids by making chimeric substitutions within this region. Renumbering the critical A subdomain amino acids 1 through 30, three chimeric AKv1.1a T1 domains were made with the following Shaw substitutions: Shaw (1-13), Shaw (14-25), and Shaw (26-30). Co-immunoprecipitation of Shaker wild type T1 domain with the Shaw (1-13) chimera shows that these two T1 domains do not heteromultimerize. There are two amino acid changes within this 13 amino acid stretch that are not found in Shaker sequences. We are now testing assembly and function of Shaker channels with point mutations in these amino acids, and examining the assembly properties of the other two chimeras.

Supported by NIH RO1-NS 31583, Baylor Mental Retardation Center P30-HD24064, Klingenstein Fellowship Award, NRSA F30 MH10511

Th-AM-G8

HIGH INTENSITY ELECTRICAL FIELD-INDUCED REDUCTION OF K CHANNEL CURRENTS MAY RESULT FROM ELECTRO-CONFORMATIONAL CHANGES IN CHANNEL'S VOLTAGE SENSORS: GATING CURRENT REDUCTION ((W, Chen and R.C. Lee)) Department of Surgery, The University of Chicago, Chicago, IL, 60637.

We have shown that high intensity electrical fields can reduce both channel's conductance and ionic selectivity of the delayed rectifier K channels (B.J. V67:603-612, 1994). The question is how the electro-conformational changes in the channel proteins cause these reductions. By measuring channel's gating currents, our experimental data support our hypothesis that the channel's voltage sensors suffer structural alternation.

Alll experiments were performed using the improved double vaseline-gap voltage clamp technique (Chen and Lee, B.J. V66:700-709) and single muscle fibers and nerve cells from frog. Both limiting equivalent number of charged particles and glob gating currents have been measured. A sequence of stimulation pulses with magnitudes around the K channel reverse potential was applied to the cell membranes pre and post shocked by two pulses of -600 mV, 4 ms, respectively. The channel conductance was normalized to the maximum value at membrane potential of +50 mV. The first three points were fitted by straight lines with a slope of e fold/4.7 mV for preshock and a slope of e fold/7.8 mV for postshock. This indicates a reduction of the channel's voltage sensitivity.

Boltzmann equation was used to calculate the minimum equivalent number of movable charges in responding to a single channel opening. At room temperature, about 5-6 particles are movable for healthy fiber and only 3 for the shocked fiber. Results from measuring glob charge movement currents are consistent with this reduction.

Reduction of number of movable charges implies an electroconformational alternation of the channel's voltage sensors. The overall effects of high intensity electrical fields on K channels lead to a larger energy barrier for the channel opening.

Th-AM-H1

RATE OF DIASTOLIC Ca RELEASE FROM THE SARCOPLASMIC RETICULUM OF INTACT RABBIT AND RAT VENTRICULAR MYOCYTES
((R.A. Bassani and D.M. Bers)) Univ Campinas, Brazil and Loyola Univ Chicago, Maywood, IL 60153.

We measured the resting unidirectional Ca efflux from the SR in intact rabbit and rat ventricular myocytes. The SR Ca content was assessed as the amount of Ca released by caffeine at different times after inhibition of the SR Ca-ATPase by thapsigargin (TG). Prior to rest intervals in Na-containing, Ca-free solution, a 3-min preperfusion with 0Na,0Ca solution was performed to deplete Na_i (aiding Ca extrusion via Na/Ca exchange) while keeping the SR Ca content constant. TG treatment was limited to the last 2 min of preperfusion with 0Na,0Ca solution to minimize SR Ca loss before addition of Na, but allowed complete block of the SR Ca pump. Total SR Ca content was estimated from the $[Ca]_i$ transient evoked by caffeine, taking into account passive cellular Ca buffering. The time constants for SR Ca loss after TG were 385 and 355 s, while the pre-rest SR Ca content was estimated to be 106 and 114 μM (μmol/l non-mitochondrial cell volume) in rabbit and rat myocytes, respectively. The initial rate of unidirectional Ca efflux from the SR was similar in these cell types (rabbit: 0.27 μM/s; rat: 0.32 μM/s, comparable with estimates from "Ca sparks", Cheng *et al.*, *Science* 262:740-744, 1993). Thus, resting leak of Ca from SR may be primarily via occasional openings of SR Ca release channels. Finally, this flux is very slow compared to other Ca transporters in ventricular myocytes.

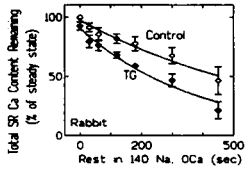

Th-AM-H2

FRACTIONAL SR Ca RELEASE IS ALTERED BY SR Ca CONTENT AND TRIGGER Ca IN CARDIAC MYOCYTES
((J.W.M. Bassani, W. Yuan and D.M. Bers)) Univ Campinas, Brazil & Loyola Univ Chicago, Maywood, IL 60153.

Release of SR Ca in cardiac E-C coupling can be graded by the amount of activating Ca outside the SR (i.e. Ca-induced Ca-release). However, little is known about how intra-SR Ca affects the release process. We assessed how the fractional SR Ca release is affected by alteration of SR Ca content and of trigger Ca (using indo-1, perforated patch to measure I_{Ca}, 10 mM caffeine to release SR Ca and thapsigargin to completely block SR Ca uptake. For "*Normal*" SR Ca load and trigger Ca (action potential with 2 mM $[Ca]_o$) 35 $\pm$ 3% of the SR Ca content was released at a twitch. Changing trigger Ca by altering $[Ca]_o$ (to 0.5 and 8 mM) at a test twitch changed this to 10 $\pm$ 2% and 59 $\pm$ 6%, with the same SR Ca load (~parallel to I_{Ca} changes from voltage clamp). Three different levels of SR Ca load were studied (Low, Normal and High) using the standard trigger Ca. The High load condition only increased SR Ca content by ~4%, but appeared to be very close to the limiting SR Ca capacity. The fractional SR Ca release increased from 3.6 $\pm$ 0.8% to 35 $\pm$ 3% to 59 $\pm$ 8% for Low, Normal and High loading conditions. We conclude that increasing SR Ca content increases Ca release both because there is a greater pool of Ca to be released, but more quantitatively important is the larger proportion of that Ca which is released. Thus the SR Ca release mechanism is sensitive to SR Ca content and this effect can also explain spontaneous SR Ca release during Ca overload.

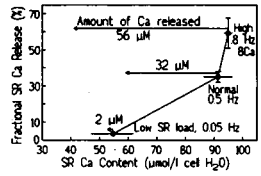

Th-AM-H3

BAY K 8644 INDUCES SHIFTS IN EXCITATION-CONTRACTION COUPLING IN FERRET CARDIAC MUSCLE.
((E. McCall & D.M. Bers)) Loyola Univ Chicago, Maywood, IL 60153.

We previously reported (*Biophys J* 66:A133, 1994) that the dihydropyridine L-type Ca channels agonist, Bay K 8644 (BAY), modifies resting SR Ca efflux in ferret ventricular muscle. In order to determine whether BAY affects *active* SR Ca efflux during E-C coupling we determined the relationship between Ca current (I_{Ca}) and contraction in patch-clamped isolated ferret cardiac myocytes at 37°C. In control solution $[Ca]_o$ was 3 mM and was reduced to 1 mM in BAY (0.1 μM), such that at the time of the test pulse the SR Ca content was comparable (based on caffeine-contracture amplitude: 10.7$\pm$3.5 μm (Control) *vs* 11.9$\pm$5.6 μm (BAY), n=6). BAY shifted the current-voltage relationship leftward, with a similar peak I_{Ca} amplitude. Despite similar degrees of SR Ca loading and Ca influx via I_{Ca}, the contraction elicited for a given I_{Ca} was much smaller in BAY (Fig). This modification with BAY occurred throughout the range of currents elicited, resulting in a downward shift of the current-contraction relationship (Fig). We conclude that while BAY increases resting efflux of SR Ca, it decreases the responsiveness of Ca-induced Ca-release during E-C coupling.

(supported in part by a British-American Research Fellowship from American Heart Association and the British Heart Foundation).

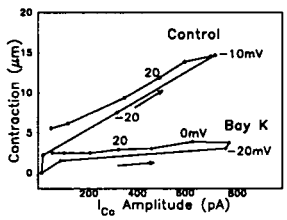

Th-AM-H4

SUMMATION OF STOCHASTIC CALCIUM SPARKS ACTIVATED BY THE LOCAL CALCIUM CHANNEL CURRENT UNDERLIES EC COUPLING IN HEART MUSCLE.

((H. Cheng, M. B. Cannell* and W. J. Lederer)) Dept. of Physiology, Univ. of Maryland, Baltimore, MD 21201 and * Dept. of Pharmacology, St. George's Hospital Medical School, London, UK

The calcium-induced calcium release mechanism amplifies calcium influx into the cell by activating the release of calcium from the SR via calcium-release channels (ryanodine receptors) to provide sufficient calcium to activate contraction during cardiac EC coupling. Elementary SR Ca-release events have been imaged using a confocal laser-scanning microscope and single heart muscle cells loaded with the calcium-sensitive indicator fluo-3 (Cheng et al, *Science* **262**, 740(1993)). Stochastic activation of SR Ca-release sites by I_{Ca} is supported by examination of the spatial non-uniformities of $[Ca^{2+}]_i$ observed when I_{Ca} is partially inhibited (Cannell et al, *J. Physiol*, **477**: 25P, (1994)) or during the rising phase of the $[Ca^{2+}]_i$ transient triggered by the action potential (Cannell et al. *Biophysical J.* In Press. (1994)). Thus local EC coupling is quite different from that inferred from the whole cell $[Ca^{2+}]_i$ measurement. We report here that by imaging $[Ca^{2+}]_i$ with an identical system under voltage-clamped conditions, we provide additional evidence that the elementary events of EC coupling are under local control of the sarcolemmal calcium influx mechanisms (e.g. I_{Ca}) as first suggested by Niggli & Lederer (*Science* **250**: *565* (1990)) and can be visualized as calcium sparks. Furthermore we show that summation of elementary, stochastic SR calcium release events (evoked "calcium sparks") can explain graded behavior of the macroscopic $[Ca^{2+}]_i$ transient.

Th-AM-H5

EVOKED CALCIUM SPARKS IN VOLTAGE-CLAMPED HEART CELLS.
((J.R. López-López, P.S. Shacklock, C.W. Balke and W.G. Wier)) University of Maryland at Baltimore, MD 21021.

We used confocal microscopy to test the hypothesis that electrically evoked $[Ca^{2+}]_i$-transients in mammalian cardiac cells are composed of stereotypical subcellular local events (*viz.* Ca^{2+}-release from one or a cluster of ryanodine receptors). Such events (previously termed evoked local $[Ca^{2+}]_i$-transients[1] or evoked Ca^{2+}-sparks) may be induced by a locally high $[Ca^{2+}]_i$ produced by a co-associated L-type Ca^{2+}-channel. We voltage-clamped single rat and guinea-pig cardiac ventricular cells that were perfused internally with two fluorescent Ca^{2+}-indicator dyes (fura-red, 100 μM; fluo-3, 50 μM) and line-scan images of evoked local $[Ca^{2+}]_i$-transients were obtained by confocal microscopy as described previously[1]. At all clamp-pulse potentials (-30 mV to +80 mV) cadmium ions (Cd^{2+}) reduced the spatial average $[Ca^{2+}]_i$-transients but revealed evoked Ca^{2+}-sparks, presumably by reducing the probability of L-type Ca^{2+}-channel opening. The voltage-dependence of the probability of occurrence of the evoked Ca^{2+}-sparks is bell-shaped, similar (but not necessarily identical) to that of the macroscopic Ca^{2+}-current or to that of the overall SR Ca^{2+}-release flux ($F_{SR,rel}$) as we have measured it previously[2]. Evoked Ca^{2+}-sparks occurred at different, but not all the possible subcellular locations in different pulses to the same membrane potential.

(1) Lopez-Lopez *et al.*, (1994). *The Journal of Physiology*, vol. 480.1, pp. 21-29.
(2) Wier *et al.*, (1994). *The Journal of Physiology*, vol. 474, pp. 463-471.

Th-AM-H6

CROSS-TALK BETWEEN Ca^{2+}-RELEASE AND INACTIVATION OF L-TYPE Ca^{2+} CHANNEL IN RAT VENTRICULAR MYOCYTES.
((S. Adachi-Akahane, L. Cleemann and M. Morad)) Department of Pharmacology, Georgetown University, Washington, DC 20007.

Calcium-mediated cross-signaling between DHP- and ryanodine-receptors was examined in rat ventricular myocytes dialyzed with high concentration of Ca^{2+}-buffers. Intracellular dialysis with 2mM Fura-2 decreased I_{Ca}-activated Ca^{2+}-transients from 500 to 50nM and abolished contraction, but the amount of Ca^{2+} released from the SR was nearly constant (150μM). 5mM caffeine applied at various times relative to the depolarizing pulse had two effects on I_{Ca} and Ca_i-transients. Activation of I_{Ca} coinciding with caffeine-induced Ca^{2+} release resulted in enhanced Ca_i-transients and inactivation of I_{Ca}. In contrast, I_{Ca} activated 300-1000ms following the Ca^{2+} release by caffeine inactivated slowly, was of similar magnitude and caused little additional release. Dialysis with 14mM EGTA and 2mM Fura-2 did not abolish the dual effects of caffeine on I_{Ca} and Ca_i-transients. Caffeine-activated $I_{Na\text{-}Ca}$, measured consistently with 0.2mM Fura-2, was absent in cells dialyzed with 2mM Fura-2. Depletion of the SR by thapsigargin significantly decreased the rate of inactivation of I_{Ca} and abolished the dual effects of caffeine on I_{Ca}. These results indicate that Ca^{2+} release from the SR continues to regulate the gating kinetics of Ca^{2+} channel even when global myoplasmic [Ca] is highly buffered suggesting that the DHP and ryanodine receptors are coupled via microdomains of Ca^{2+}. Supported by NIH HL16152.

Th-AM-H7

EVIDENCE FOR A Ca^{2+}-ACTIVATING SITE IN OR NEAR THE CONDUCTION PATHWAY OF THE SKELETAL MUSCLE Ca^{2+}-RELEASE CHANNEL. ((A. Tripathy and G. Meissner)) Dept. of Biochemistry & Biophysics, University of North Carolina, Chapel Hill, NC 27599-7260. (Spon. by Qi-Yi Liu)

The effect of lumenal (trans) Ca^{2+} on Ca^{2+}-release channel activity was investigated at low cytoplasmic (cis) Ca^{2+} after incorporation of purified RyR into planar bilayer membranes using K^+ as current carrier. Channels activated by 5 mM cis ATP in presence of nM cis and 0.05-10 mM trans Ca^{2+}, exhibited a profound voltage-dependence of activation and gating. At 50 μM trans Ca^{2+} and -ve potentials (trans as ground) P_o was 5-10 times higher and the duration of open events much longer than at +ve potentials. Channel activity increased in a dose-dependent manner at -ve potentials as trans [Ca^{2+}]was raised from ≈1 μM to ≈1 mM beyond which the activity started to decline. Simultaneously, increased channel activity and long duration open events started appearing at +ve potentials. At increasingly +ve applied potentials higher trans [Ca2+] were necessary to activate the channel. Addition of fast Ca^{2+}-complexing buffer (BAPTA,10 mM) to the cis side further increased channel activity. Increased channel activity was abolished if trans [Ca^{2+}] was lowered to <1 μM and the effects of trans Ca^{2+} could not be replaced by other divalent ions like Ba^{2+} or Mg^{2+}. These results suggest that Ca^{2+} flowing through the channel (trans ⇒ cis) activate and inactivate the channel. The effect of BAPTA suggests that the activating site is located in or near the conduction pathway and that the cis inactivating site may lie farther away.

Th-AM-H8

ADAPTATION REGULATES THE PHYSIOLOGICAL RESPONSE OF THE CARDIAC RYANODINE RECEPTOR TO CALCIUM. *((H. H. Valdivia[1], J. H. Kaplan[3], G. C. R. Ellies-Davies[3] and W. J. Lederer[2])) University of Wisconsin-Madison[1], University of Maryland-Baltimore[2], and Oregon Health Sciences University[3].*

Adaptation is a fundamental feature of sarcoplasmic reticulum calcium release channels (RYR). It permits successive increases of Ca^{2+} to repeatedly but transiently activate RYRs (Györke and Fill, *Science* **260**:807). It was suggested that adaptation could be the mechanism that turns off Ca^{2+}-induced Ca^{2+} release *in vivo*, but the rate of adaptation measured in simplified solutions was too slow to be of physiological significance. Photorelease of Ca^{2+} from nitrophenyl-EGTA, a novel photolabile Ca^{2+} chelator, shows that adaptation in the absence of Mg^{2+} is indeed an extremely slow process (1.35 s, D-a). After 1 mM [Mg^{2+}] was added, peak P_o decreased and the rate of adaptation increased to 98 ms (D-b). A larger [Ca^{2+}] step to 10 μM was required to increase the peak P_o, but the rate of adaptation was still fast (168 ms, D-c). Thus, physiological [Mg^{2+}] shifts the threshold of RYR Ca^{2+} activation to higher [Ca^{2+}] and accelerates its adaptation to a rate comparable to that seen for the decay of the intracellular [Ca^{2+}] transient in intact cells. Additionally, phosphorylation of RYR by PKA increases the responsiveness and accelerates the kinetics of adaptation (not shown). Thus, adaptation may be in fact kinetically relevant for heart cells under physiological conditions. Supp. by NIH & AHA

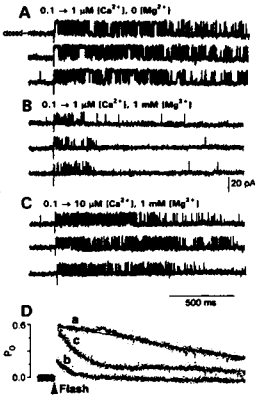

Th-AM-H9

TWO DIFFERENT Ca^{+2}-DEPENDENT NEGATIVE CONTROL MECHANISMS REGULATE SINGLE SKELETAL RYANODINE RECEPTOR CHANNELS. ((Velez, P., S. Györke* and M. Fill)) Dept. Physiology, Univ. Texas Medical Branch, Galveston TX, 77555-0641 and *Dept. Physiology, Texas Tech University, Lubbock TX, 79430.

Single dog cardiac and skeletal muscle ryanodine receptor (cRyR & sRyR) channels were reconstituted in planar bilayers. Fast calibrated Ca^{+2} stimuli were applied by laser flash photolysis of DM-nitrophen, a caged-Ca^{+2} compound. Intense UV light was applied to a small volume of solution directly in front of the bilayer through a micropositioned optic fiber. Solutions contained (in mM): 250 $CsCH_3SO_3$, 10 CsHEPES (pH 7.4) and 2 DM-nitrophen. The free [Ca^{+2}] was carefully titrated to pCa 7 and continuously monitored by a Ca^{+2} electrode. In parallel experiments, photolytic Ca^{+2} stimuli were calibrated by a Ca^{+2} microelectrode & microfluorimetry. Channel activity was analyzed by generation of ensemble currents. Fast sustained photolytic Ca^{+2} steps (pCa 7→6) activated both cRyR and sRyR channels. While free [Ca^{+2}] was elevated, channel activity (Po) peaked then spontaneously decayed (time constant, τ=0.98 s for cRyR; τ=4.18 s for sRyR). The slow decay of sRyR activity may be due to Ca^{+2} adaptation as defined in cRyR (Science 260:807-,1993). Once maximally activated by high [Ca^{+2}], a fast Ca^{+2} step to a higher [Ca^{+2}] did not alter cRyR activity. A fast Ca^{+2} step applied to a maximally activated sRyR induced a rapid ($\tau \approx 300$ μs) decrease in Po (fast inactivation). Thus, two separate Ca^{+2}-dependent negative control mechanisms (adaptation/fast inactivation) may regulate the sRyR channel.

NUCLEIC ACIDS

Th-AM-I1

DNA ATTRACTION BY CORRELATED COUNTERION FLUCTUATIONS. ((I.F. Rouzina & V.A. Bloomfield)) Biochem, U of Minn, St. Paul MN 55108

Electrostatic correlation of fluctuations of multivalent counterions can drive DNA collapse from dilute solution. A thin layer near each DNA surface contains most of the screening ions. Coulomb repulsion between ions in a layer produces lateral ordering, resulting in an alternating surface charge pattern. The mobile charges on apposing surfaces can adjust to complement each other, producing an attractive force. The attractive energy has maximum value $W_C = (ze)^2/a\varepsilon$, a is the average lateral distance between counterions of valence z, $(n_2/z)^{-1/2}$, and n_2 is the surface charge density. It is reduced by lateral thermal disordering of the ions. The range of both effects is O(a). We quantify this effect by calculating the total free energy of interaction vs intersurface separation. At $W_C/k_BT > 4$ an abrupt transition to the collapsed state occurs. In water at room temperature, this condition can be achieved only with $z \geq 3$, in accord with experiment. Out-of-plane thermal ion motion provides a "hard wall" repulsion at a few Å separation which, probably together with hydration forces, keeps the DNA molecules from complete fusion. The binding free energy and equilibrium separation then are functions of W_C/k_BT. We calculate pressure vs separation curves for various W_C/k_BT ratios for comparison with osmotic stress measurements by Rau & Parsegian (1992) as a function of [$Co(NH_3)_6^{3+}$].The variation in W_C with amount of $Co(NH_3)_6^{3+}$ at the DNA surface seems to account, without adjustable parameters, for the transition from purely repulsive through precritical to attractive interaction. The theory also accounts for the ability of divalent cations to condense DNA at lower dielectric constant ε.

Th-AM-I2

TRANSIENT ELECTRIC BIREFRINGENCE OF KILOBASE-SIZED DNA MOLECULES. ((Nancy C. Stellwagen)) Department of Biochemistry, University of Iowa, Iowa City, IA 52242

Circular, kilobase-sized DNA molecules exhibit electrophoretic mobilities that depend on the site of linearization, suggesting that large DNAs contain discrete sites which are stably curved or bent. In this study, the electric birefringence of several linearized, permuted pBR322 and SV40 DNA molecules has been measured. The terminal relaxation times of both DNAs depend on the site of linearization, suggesting that their conformations in solution depend on base sequence. For both DNAs, the longest terminal relaxation times are observed for DNAs linearized at the major bend center identified by the circular permutation assay, suggesting that this site is indeed the site of maximum curvature. Supported in part by NIH grant GM29690.

Th-AM-I3

DYNAMICS OF POLY(dA-dT)•POLY(dA-dT) STUDIED BY TIME-RESOLVED INTRINSIC FLUORESCENCE. ((Solon Georghiou[1], Joseph M. Beechem[2] and Thomas D. Bradrick[1])) [1]Molecular Biophysics Lab., Physics Dept., University of Tennessee, Knoxville, TN 37996 and [2]Dept. of Molecular Physiology and Biophysics, Vanderbilt University, Nashville, TN 37232.

There is considerable interest in delineating the conformational flexibility of the double helix of DNA because of the role this property plays in its diverse functions. These include the enzymatic recognition of specific DNA sequences, the control of genes from a distance, the interaction of different types of drugs with DNA, the packaging of DNA into chromosomes, and the formation of photodefects in DNA. Several recent molecular dynamics simulation studies for fully hydrated oligonucleotides, reported in the literature on the picosecond scale, have detected large root-mean-square deviations from the initial structures, with the bases attaining inclined positions relative to the perpendicular to the helix axis. We have studied the dynamics of the alternating polynucleotide poly(dA-dT)•poly(dA-dT) in a 50 mM cacodylate, 0.1 M NaCl, pH 7 buffer by using the time-correlated picosecond anisotropy of thymine (excitation at 293 nm). The anisotropy for monomeric emission, monitored at 340 nm, reveals large-amplitude fast motional modes and decays to a value of about 0.1 in 10 ns. Addition of 77% sucrose by volume greatly decreases the rate of the decay of the fluorescence anisotropy. Conversely, the decay rate is greatly increased upon melting of the polynucleotide at 75°C. These observations, which are very similar with those we previously made for the nonalternating polynucleotide poly(dA)•poly(dT), strongly support the motional origin of the observed fluorescence depolarization. The anisotropy for excimeric emission at 440 nm exhibits an associative behavior and decays to a value of about 0.06 in 1 ns. This work was supported by NIH Research Grant GM38236 (to SG). JMB is an L. P. Markey Scholar.

Th-AM-I4

DNA BENDING AND "STRUCTURAL" WATERS IN THE MAJOR GROOVE OF A_n:T_n TRACTS. A MONTE CARLO SIMULATION. ((A.V. Teplukhin, V.I. Poltev, R.L. Jernigan and V.B. Zhurkin)) Lab. of Matematical Biology, NCI, NIH, Bethesda, MD 20892.

The hydration of various conformations of the AT-containing decamers was analyzed by Monte Carlo calculations. In agreement with previous studies, the strongest hydration was observed for the conformations with the narrowest minor groove, which are known to cause DNA curvature when surrounded by GC-rich sequences. However, in contrast to the common belief, the advantage of such conformations is related mainly to the hydration of the Major groove rather than to the minor groove. The energy of hydration of the bases in the Major groove varies within 4 kcal/mol base pairs, but only within 1 kcal/mol in the minor groove. When the minor groove is compressed and the Major groove is opened wider, the Major groove hydration shell of the AA steps contains "structural" water molecules hydrogen bonded to three hydrophilic centers simultaneously ("trident waters"). The three centers are: two N7 atoms of adjacent adenines and one amino-proton H(N6).
A new concept is proposed, linking the phenomenon of the low-temperature intrinsic curvature of DNA to the formation of the novel hydration spine in the major groove of the An:Tn fragments.

Th-AM-I5

THERMODYNAMIC CHARACTERIZATION OF BPDE-DNA COMPLEXES ((Luis A. Marky[1], Dionisios Rentzeperis[1], Natasha Lounova[1], Nicholas E. Geacintov[1], and Donald W. Kupke[2])) [1]Department of Chemistry, New York University, New York, NY 10003; and [2]Department of Biochemistry, University of Virginia, Charlottesville, VA 22908.

We used a combination of spectroscopy, calorimetry and density techniques to characterize the thermodynamics of placing covalently bound hydrophobic moeities in the minor groove of DNA undecamer duplexes. We used the control duplex d(CCATCG*CTACC)/d(GGTAGCGATGG) and two adducts in which the enantiomers (-)-BPDE and (+)-BPDE of trans-7,8-dihydroxy-anti-9,10-epoxy-7,8,9,10-tetrahydrobenz[*a*]pyrene are bound covalently to N^2 of the G*. The (-)-BPDE-DNA and (+)-BPDE-DNA complexes melt with transition temperatures 4.6 and 8.4°C lower than the unmodified duplex, respectively. At 20°C, this corresponds to unfavorable $\Delta\Delta G°$ terms of 1.9 and 4.4 kcal/mol that result from the partial compensation of unfavorable $\Delta\Delta H$ terms of 7.4 and 16.6 kcal/mol with favorable $\Delta(T\Delta S)$ terms of 5.5 and 13 kcal/mol, respectively. These differential compensations correlated with the differential volume expansions of the complexes. Correlation of the thermodynamic data with structural data of the BPDE-DNA complexes suggests that the differential thermodynamic parameters, together with the similar values for the uptake of counterions, correspond to a differential hydration of the specific atomic groups of BPDE that are exposed to solvent while in the minor groove of B-DNA. Supported by Grants GM-42223, GM34938 and CA20851 from the NIH.

Th-AM-I6

A PYROPHOSPHATE LINKAGE AS A PROBE OF REPAIR ENZYME RECOGNITION OF SINGLE BASE LESIONS IN DNA. A MOLECULAR MODELING STUDY. ((M.P. Glackin, A.A. Purmal, S.S. Wallace and Y. W. Kow)) Department of Microbiology and Molecular Genetics, Markey Center for Molecular Genetics, University of Vermont, Burlington, VT

Introduction of a synthetic pyrophosphate linkage (PP) into DNA immediately 5' or 3' to an abasic site or a uridine residue greatly reduces or, for some enzymes, completely eliminates removal of these species by the appropriate DNA repair enzymes (A. Purmal & Y.W. Kow, in preparation). Although differences in the catalytic activity of different repair enzymes in the presence of a PP linkage have been noted, this inhibition does not appear to be correlated with the location of the linkage 5' or 3' to the lesion or with the type of endonuclease (5' or 3') involved. A PP linkage is known to affect neither the thermal nor pH stability of DNA, suggesting that the DNA is not greatly altered by this linkage. To assess the structural features in DNA containing a PP linkage which affect enzyme recognition and cleavage, canonical B DNA 15mers containing a PP linkage 5' or 3' to an abasic site and uridine were constructed and exhaustively energy minimized (RMS derivative <0.001kcal/Å) in Discover 2.8 (Biosym Corp.) using AMBER potentials and charges, with partial charges for the PP linkage developed in MOPAC.
These calculations suggest that a PP linkage introduces distortions in the DNA structure immediately adjacent to the PP, particularly 5' , and that magnitude of these distortions is highly dependent on the sequence immediately surrounding the linkage. Changes in the propeller and open values for base pairs are correlated with the position of the PP linkage, while the increases in buckle and distance appear to be sequence specific. Increases in the roll and twist values are observed 5' to the linkage, while tilt and shift are increased on both sides of the PP. Incline of the individual bases is increased for the bases on the strand opposite the linkage and incline of the base pairs is increased 5' to the linkage site. This local distortion may slow recognition of the lesions by repair enzymes. The additional backbone atoms of the PP group tend to partially block the major groove which may affect binding of the enzymes.

Th-AM-I7

MULTIPLE FLUORESCENCE LIFETIMES FOR OLIGONUCLEOTIDES CONTAINING SINGLE, SITE-SPECIFIC MODIFICATIONS AT GUANINE AND ADENINE ARISING FROM ADDITION OF 7,8-DIHYDROXY-9,10-EPOXY-7,8,9,10-TETRAHYDROBENZO[A]PYRENE. ((P. R. LeBreton[†], C.-R. Huang[†], H. Fernando[†], B. Zajc[‡], M. K. Lakshman[‡], J. M. Sayer[‡] and D. M. Jerina[‡])) Department of Chemistry[†], The University of Illinois at Chicago, Chicago, IL 60607-7061, and Laboratory of Bioorganic Chemistry[‡], NIDDK, The National Institutes of Health, Bethesda, MD 20892. (Spon. L. Kar)

Fluorescence decay profiles have been measured for four oligonucleotide duplexes
$^{5'}$GGT CA*C GAG$^{3'}$ ([+] and [-] ***trans*** **I**) and
$^{3'}$CCA GG G CTC$^{5'}$

$^{5'}$CCA TCG*CTA CC$^{3'}$ ([+] and [-] ***trans*** **II**)
$^{3'}$GGT AGC GAT GG$^{5'}$
in which an exocyclic amino group of deoxyadenosine (A*) or deoxyguanosine (G*) has been alkylated by *trans* opening at C-10 of the epoxide group of either the (+)-(*R,S,S,R*)- or (-)-(*S,R,R,S*)-enantiomer of (±)-7β,8α-dihydroxy-9α,10α-epoxy-7,8,9,10-tetrahydrobenzo[a]pyrene (BPDE in which the benzylic 7-hydroxyl group and the epoxide oxygen are *trans*). All of the profiles exhibit at least three fluorescence lifetimes at 15 °C. Two of the lifetimes are short (0.5 to 14 ± 1 ns) and one is long (35 to 59 ± 3 ns). When compared to fluorescence decay profiles of the modified, single-stranded oligonucleotides ([+] and [-] ***trans*** **SS-I**, and [+] and [-] ***trans*** **SS-II**) and of the *cis* and *trans* opened products formed on alkylation at the 6-amino group of 2'-deoxyadenosine 5'-phosphate by (+)-(*R,S,S,R*)-BPDE ([+] ***trans*** and [+] ***cis*** **A**) the decay profiles for the double-stranded oligonucleotide adducts provide evidence that all four of these adducts occur in multiple conformations.

Th-AM-I8

PHOTOELECTRON AND QUANTUM MECHANICAL DESCRIPTION OF IONIZATION POTENTIALS OF Na^+-WATER-2'-DEOXYGUANOSINE 5'-PHOSPHATE CLUSTERS: ELECTRONIC INFLUENCES ON DNA ALKYLATION. ((H. S. Kim and P. R. LeBreton)) Department of Chemistry, The University of Illinois at Chicago, Chicago, IL 60607-7061. (Spon. by S. Hanlon)

UV photoelectron spectra of 1,9-dimethylguanine, 3-hydroxytetrahydrofuran, and water, and results from quantum mechanical, self-consistent field (SCF) and post-SCF calculations were employed to describe the valence electronic structures of clusters containing 2'-deoxyguanosine 5'-phosphate (5'-dGMP$^-$), 4 water molecules and a phosphate-bound sodium ion. Two cluster geometries (A and B) were examined. In (A), the Na^+ counterion is coordinated to 5'-dGMP$^-$. In (B), the Na^+ ion and 5'-dGMP$^-$ are separated by water. In the 5'-dGMP$^-$ clusters, the energetic ordering of nucleotide ionization potentials (IPs) is different from that reported earlier for isolated 5'-dGMP$^-$. The lowest energy IP in isolated 5'-dGMP$^-$ (4.6 eV) arises from the phosphate group; the lowest energy IPs in A (8.2 eV) and B (7.9 eV) arise from the base. In A and B, the smaller IP of the base, compared to the phosphate group, suggests that in electrophilic S_N2 attack by carcinogenic methylating and ethylating agents, activation barriers are strongly influenced by base polarizabilities. This is consistent with the finding that in DNA and RNA reactions with N-methyl-N-nitrosourea, dimethyl and diethyl sulfate, and methyl and ethyl methanesulfonate more than 75% of nucleotide alkylation occurs at the bases.

Th-AM-I9

HPLC PREPARATION OF HIGHLY PURIFIED SINGLE-STRANDED M13 DNA. ((A. Milliman, C.-R. Huang, Y. Kim and P. R. LeBreton)) Department of Chemistry, The University of Illinois at Chicago, Chicago, IL 60607-7061.

Closed-circular, single-stranded viral DNA is frequently employed in DNA cloning and sequencing experiments. Because circular, single-stranded viral DNA has a well defined structure and sequence, this structural form of DNA has also been employed in ligand binding experiments and other biophysical measurements. However, there is an high molecular weight impurity, observed in light scattering experiments, that sometimes contaminates single-stranded DNA purified from phage which has been precipitated in poly(ethylene glycol) (PEG (8000)), and purified by standard phenol-chloroform extraction. Three methods were investigated which remove the polymeric impurity from closed-circular, single-stranded M13mp19 DNA (SS M13 DNA). One employs a commercial preparation and yields pure SS M13 DNA, as shown by light scattering measurements. However, analysis by high performance liquid chromatography (HPLC) indicates that the commercial preparation results in DNA degradation. Another method employs a Whatman DE52 (diethylamino cellulose) column. This procedure yields intact DNA, but in poor yield (less than 20% of that obtained by phenol-chloroform extraction). The last method was the most successful. This method employs HPLC with a Waters AP-1 column with 8h DEAE bedding. The HPLC procedure provides DNA in high yield (80-90% column recovery) with an intact structure. This is an efficient method for the isolation of high purity, closed-circular, single-stranded viral DNA suitable for physical measurements.

MUSCLE REGULATORY PROTEINS

Th-AM-J1

CALCIUM BINDING EFFECTS ON STRUCTURE AND DYNAMICS OF TROPONIN C: FLUORESCENCE DECAY OF A TRP MUTANT ((D.S. Gottfried*, J.M. Friedman*, V.G. Rao#, and J. Gulati#)) Depts. of Physiology and Biophysics* and Medicine#, Albert Einstein College of Medicine, Bronx, NY 10461.

Troponin C (TnC), a Ca^{+2}-receptor protein important in the triggering of thin filament-mediated muscle contraction, contains 4 EF-hand binding sites separated by a long α-helix. A single tryptophan introduced near the Ca^{+2} binding loop of site I in rabbit skeletal TnC (sTnC.F26W) provides a convenient spectroscopic probe. Steady-state and time-resolved fluorescence measurements were used to measure Ca^{+2}-dependent flexibility and structural relaxation. Steady-state fluorescence shows a four-fold increase in quantum yield and 2.5 nanometer blue shift upon Ca^{+2} binding. This is consistent with a large structural change in the tryptophan region accompanied by a change in polarity of the environment around the indole ring. Lifetime measurements confirm the Ca^{+2}-dependent quenching mechanism as containing both static and dynamic components, and structural models of the Ca^{+2}-loaded protein indicate methionine 45 as a potential candidate for the quenching moiety. A decrease in the number of required fitting terms from three to two (with 96% of the fluorescence from a single component) indicates an increase in structural homogeneity with Ca^{+2} binding. Interpretation of wavelength-dependent lifetimes are complicated by competing effects of dielectric relaxation (τ increases with λ) and ground-state heterogeneity (τ decreases with λ); however, results indicate that Ca^{+2} binding significantly suppresses dielectric relaxation around the photoexcited tryptophan. These observations are consistent with a functional model in which signaling efficiency is enhanced through increased protein rigidity and decreased structural dynamics.

Th-AM-J2

Nebulin Fragment Binds Both S-1 and Actin, and Prevents Binding to Actin. ((Douglas D. Root & Kuan Wang)) Department of Chemistry and Biochemistry, University of Texas at Austin, Austin, Texas 78712, (spon. by A. Brady).

We have previously shown that bacterially expressed human nebulin fragments form a complex with calmodulin in solution and act as a calcium-mediated regulatory system of actomyosin filament sliding and ATPase (Root and Wang, 1994, "Calmodulin-sensitive interactions of human nebulin fragments with actin and myosin," **Biochemistry 33**, in press). We have now proceeded to study the molecular interactions of actin and myosin in the presence of nebulin fragment NA3 with fluorescence spectroscopy by monitoring fluorescence of actin labeled with pyrene on Cys374. Under rigor conditions, binding of S-1 to actin rapidly reduces fluorescence by 70%. This fluorescence quenching is inhibited by NA3 when NA3 is premixed with F-actin, prior to S-1 addition. Longer incubation (1-2 hrs.) of this mixture, however, led to a gradual quenching to a level approaching that of acto-S-1 complex alone. If NA3 is added to pyrene-actin that has been premixed with S-1, then only a slight elevation of the quenched fluorescence (5-10%) is observed. These results indicate that NA3 inhibits binding of S-1 to F-actin under rigor conditions.
The effects of NA3 on S-1 and actin interactions in the presence of ATP is more complex. When NA3 is mixed with acto-S-1 prior to adding ATP, the fluorescence increases rapidly upon dissociation of S-1 from actin, and then decreases slowly during steady state hydrolysis of ATP. NA3 affects both the rate and extent of fluorescence quenching during steady-state ATP hydrolysis. When ATP is hydrolyzed completely, the fluorescence plateaus at levels that are higher in the presence of NA3, indicating an inhibition of the binding of ADP-S-1 to actin by NA3. These results are being analyzed by a model in which NA3 simultaneously binds S-1 and actin but holds them apart so that activation of ATPase by actin is inhibited. (Supported by MDA and NIH).

Th-AM-J3

Single Nebulin Superrepeat Affects Multiple Actin Protomers in Actomyosin Interaction and Actin Polymerization. ((Douglas D. Root & Kuan Wang)) Department of Chemistry and Biochemistry, University of Texas at Austin, Austin, Texas 78712.

Nebulin has been proposed to be a calcium-calmodulin mediated regulatory protein along the entire length of the thin filaments of skeletal muscles (Root and Wang, 1994, "Calmodulin-sensitive interactions of human nebulin fragments with actin and myosin," **Biochemistry 33**, in press). To explore the molecular mechanisms of the effect of nebulin on actomyosin interaction, we studied in detail a bacterially-expressed human nebulin fragment, NA3 (eight module). The binding stoichiometry of NA3 to actin and its effects on actin-activated S-1 ATPase activities were measured under similar conditions. NA3 binds to F-actin with a dissociation constant 1.2±0.2 μM and a stoichiometry of one NA3 per actin protomer. NA3 also binds to S-1. However, since S-1 does not inhibit NA3 binding to actin in the presence of ATP, it is therefore possible to calculate the amount of actin-bound NA3 under the conditions of ATPase assays. A positive correlation exists between the ratio of bound NA3 and the degree of inhibition of actin activated S-1 ATPase. There was no correlation between the degree of NA3 bound per S-1 and the inhibition of acto-S-1 ATPase. We conclude that the binding of NA3 to actin is critical for the inhibition of actomyosin ATPase. Further analysis of the inhibition curve suggests that each bound NA3 may prevent multiple (2-3) actin protomers from activating S-1 ATPase. To evaluate this hypothesis, the effect of NA3 on actin polymerization was investigated by monitoring enhancement of the pyrene-actin fluorescence upon polymerization. The fraction of polymerized actin was consistently 2-3 times that of the calculated fraction of actin bound by NA3. Our data suggest that one superrepeat of nebulin contains one high affinity actin binding site, but can exert influence on multiple actin protomers. The nebulin superrepeat might exhibit additional lower affinity contacts with multiple actin protomers or alternatively, a single high affinity actin binding site might induce conformational changes which are transmitted to neighboring actin protomers. (Supported by MDA and NIH).

Th-AM-J4

PROBING THE BINDING STABILITY AND ACTIVATION PROPERTIES OF TROPONIN C USING CALMODULIN[TROPONIN C] CHIMERAS ((F. Schachat†, S.E. George‡, and P.W. Brandt*)) Department of Cell Biology† and Departments of Medicine and Pharmacology‡, Duke University Medical Center, Durham, NC 27710, and Department of Anatomy and Cell Biology*, Columbia University School of Medicine, New York, New York, 10032.

The high affinity divalent metal ion binding domains III and IV of troponin C (TnC) stabilize the association of TnC with the thin filament calcium regulatory complex. By substituting these domains separately for the corresponding low affinity calcium-specific domains in calmodulin (CaM) in the CaM[TnC] chimeras CaM[3 TnC] and CaM[4 TnC], we have investigated whether both are needed for stable association with the thin filament calcium-regulatory complex. The difference in stability (assessed by the off rate at pCa 8) indicates that these two domains form a functional unit under relaxing conditions, as both are required for stable association of the chimera with the thin filament. However, when the thin filament regulatory complex is activated, at pCa 4, either of the two C-terminal high affinity divalent metal ion binding sites is sufficient for stable association. The difference in behavior between CaM and CaM[3TnC] and CaM[4 TnC] under activating conditions is interesting because studies on the affinity of these proteins for divalent metal ions in solutions indicates that all binding sites should be occupied at pCa 4. Investigations of other chimeras reveals that domains required for calcium-activation of contraction can be separated from those needed for cooperative activation of the thin filament regulatory strand.

Th-AM-J5

STRUCTURAL DETAILS OF A CALCIUM INDUCED MOLECULAR SWITCH: COMPARISON OF THE HIGH RESOLUTION, X-RAY CRYSTALLOGRAPHIC STRUCTURES OF THE CALCIUM-FILLED AND CALCIUM-FREE FORMS OF THE N-TERMINAL REGULATORY DOMAIN OF TROPONIN C. ((N.C.J. Strynadka, M. Chemaia, M. Li, L.B. Smillie and M.N.G. James)) The MRC Group in Protein Structure and Function, Department of Biochemistry, University of Alberta, Edmonton, Alberta, Canada, T6G 2H7

The binding of calcium ions to the N-terminal regulatory domain of troponin C elicits a conformational change which constitutes the major intracellular signal for the initiation of muscle contraction (1). Due to the low pH of the crystallization media, the original x-ray crystallographic structure of troponin C (2,3) had the N-terminal domain in the calcium-free state. Recently the N-terminal domain of chicken skeletal TnC has been cloned, expressed (4) and crystallized at pH 7.5. The x-ray crystallographic structure of the calcium loaded N-terminal domain has been solved to high resolution (1.6 Ang.). A detailed comparison of the molecular changes in the calcium free and calcium filled state of the domain will be discussed.

1) Zot, A.S., and Potter, J.D. 1987 Ann. Rev. Biophys. Biophys. Chem. 16:535-559
2) Herzberg, O. and James, M.N.G. 1985 Nature 313:653-659
3) Sundarlingam, M. *et al.* 1985 Science 227:945-948
4) Li, M.X., Chandra, M., Pearlstone, J., Racher, K.I., Trigo-Gonzalez, G., Borgford, T., Kay, C.M., and Smillie, L.B. 1994 Biochemistry 33 917-925

Th-AM-J6

CALMODULIN HAS AN EXTENDED CONFORMATION WHEN COMPLEXED WITH SMOOTH MUSCLE CALDESMON. ((Y. Mabuchi, C.-L.A. Wang & Z, Grabarek)) Muscle Research Group, Boston Biomedical Research Institue, Boston, MA 02114.

CaM34/110 is a mutant of human liver calmodulin with Cys residues substituted for Thr34 and Thr110. The global conformation of CaM34/110 can be monitored by energy transfer between a donor (AEDANS, N-iodoacetyl-N'-(5-sulfo-1-naphthyl)ethylenediamine) and an acceptor (DAB, 4-dimethyl -aminophenylazophenyl-4'-maleimide) attached to the Cys residues. Upon complex formation between CaM34/110-AEDANS/DAB and caldesmon (CaD) there is an increase in the AEDANS fluorescence intensity indicating an increase in the average distance between the probes. The C-terminal 22 kDa recombinant fragment of CaD (residues 579-756) is also capable of inducing a similar increase in the fluorescence of CaM34/110-AEDANS/DAB, however the three short synthetic peptides of CaD corresponding to the putative CaM binding sites: GS17C (651-667), MG56C (658-713) and VG29C (685-713) are ineffective in this respect, although they bind to CaM34/110. These results indicate that the conformation of CaM in the complex with CaD is extended, similar to that reported for free CaM (Babu et al. Nature 315,37,1985) and unlike that reported for the CaM-M13 complex (Ikura et al. Science 256,632,1992; Meador et al. Science 257,1251,1992). It appears that some stabilization of the CaM-binding regions of CaD by other parts of the C-terminal domain of CaD is necessary for their ability to induce the correct conformation in CaM. Alternatively, there may be another, yet unidentified, CaM-binding segment in the C-terminal domain of CaD which accounts for the difference in the properties of the 22 kDa fragment and the shorter peptides. (Supported by NIH, AR-41156, AR-41637)

Th-AM-J7

CALDESMON CONTROLS ACTOMYOSIN ATPASE AND FILAMENT MOTILITY BY SWITCHING ACTIN-TROPOMYOSIN FROM THE 'ON' TO THE 'OFF' STATE ((S.B. Marston and I.D.C. Fraser))
Dept. Cardiac Medicine, NHLI, Dovehouse St., LONDON SW3 6LY, UK

We compared the effect of inhibitory concentrations of caldesmon, caldesmon fragment H9 (C-terminal 69 amino acids of human caldesmon) and troponin upon the interaction of the strongly binding species S-1.AMP.PNP and NEM-S-1 with actin-smooth muscle tropomyosin (Atm) at 0.03M ionic strength. At low concentrations of S1.AMP.PNP all the inhibitors reduced afinity for ATm >20 fold and the binding curve was highly cooperative . 0.1 NEM-S-1/actin potentiated Atm activation of myosin MgATPase 6-fold. Caldesmon inhibited the ATPase in the presence and absence of NEM-S-1. NEM-S-1 reactivated Atm ATPase which had been inhibited by troponin, caldesmon or H9. Thus in solution caldesmon and troponin inhibition is associated with inhibiting strong crossbridge binding by switching the actin-tropomyosin 'on'/'off' equilibrium towards the 'off' state.
We also studied caldesmon control of Atm in an *in vitro* motility assay. Actin-smooth muscle tropomyosin moving over immobilised skeletal muscle HMM was measured at I=0.08M, 28°C in 0.5% methylcellulose. 40nM tm increased the velocity of actin filament movement from 3.46 to 4.40 μm/ sec, confirming that the smooth muscle Atm complex is predominantly in the 'on' state. Addition of caldesmon did not reduce filament velocity, however as concentration increased more and more actin filaments stopped moving. Most of the filaments stopped moving at caldesmon concentrations (25nM) which had little effect upon the number of actin filaments associated with HMM. Thus, as in solution, caldesmon inhibition involves mainly strongly bound actin-myosin complexes and is highly cooperative; a whole actin filament is switched on or off as a unit.

Th-AM-J8

CALDESMON, CALPONIN, AND TROPOMYOSIN REGULATE IN VITRO MOTILITY AND ISOMETRIC FORCE PRODUCTION BY DEPHOSPHORYLATED CROSS BRIDGES. ((J.R. Haeberle)) Dept.Molecular Physiology and Biophysics, The University of Vermont, Burlington, VT, 05405

We previously reported that the activation of isometric force by myosin light chain phosphorylation was highly cooperative for regulated thin filaments reconstituted with calponin and tropomyosin. We proposed that dephosphorylated cross bridges were being activated by "turned-on" thin filaments, and that calponin promoted the turning-on of thin filaments by slowing the dissociation rate of the high-affinity phosphorylated cross bridges. In the present study, caldesmon is shown to completely inhibit the calponin-tropomyosin-dependent recruitment of dephosphorylated cross bridges at concentrations that have no effect on force production by phosphorylated cross bridges. Isometric force production was measured using an in vitro motility assay and a simple method for measuring isometric force using NEM-modified myosin to mechanically load thin filaments. Relative changes in isometric force were measured as the minimum molar ratio of NEM-modified/unmodified myosin that halted filament motion. Force was measured as a function of the % thiophosphorylated myosin, for reconstituted thin filaments containing tropomyosin, caldesmon, and calponin. Reconstituted filaments containing saturating tropomyosin and 2 uM calponin developed approximately three times as much force as unregulated thin filaments with 100% phosphorylated myosin. In the presence of tropomyosin and calponin, the same maximum force was produced with as little as 10% thiophosphorylated myosin. The addition of 3 uM smooth muscle caldesmon under these conditions had no effect on maximum force with 100% phosphorylated myosin, but reduced force by >90% with 20% phosphorylated myosin. These findings demonstrate that caldesmon inhibits the activation of dephosphorylated cross brides by "turned-on" thin filaments, and does so at concentrations lower than those required to inhibit phosphorylated cross bridges.

NUCLEIC ACID MOTIFS FOR PROTEIN RECOGNITION

Th-PM-Sym-1

INTERACTION OF INITIATION FACTORS WITH mRNA. ((D.J. Goss))
Hunter Col., CUNY.

Th-PM-Sym-2

THE IRON REGULATORY ELEMENT (IRE) IN FERRITIN mRNA. ((E.C. Theil, H. Sierzputowska-Gracz, and R.A. M^{c}Kenzie)) **Departments of Biochemistry and Physics, North Carolina State University, Raleigh, NC, 27695-7622.**

Iron storage (ferritin) and iron uptake [transferrin receptor (TfR)] is coordinately regulated in animals by the IREs in mRNA and the IRP regulator protein, a cytoplasmic aconitase (reviewed in Theil, (1994) *Biochem. J.* 304:1-11).Low cellular iron levels enhance IRE/IRP binding to block eIF and ribosome binding (ferritin mRNA) or nuclease binding (TfR mRNA). All IREs are hairpins with a conserved terminal loop (HL), CAGUGU/C . Instability IREs with AU-rich stems, occur as five sets, each one phylogenetically conserved in the 3'-UTR. Translation IREs (erythroid aminolevulinate synthase and ferritin) have more G/C-rich stems and are in the 5'-UTR near the cap. The ferritin IRE is functionally distinct; it is more efficient and encoding both translation enhancement and repression. Structural distinctions of the ferritin IRE include an internal loop , rather than a bulge, and a base paired flanking region with a conserved triplet of base pairs (TBP) 11 nucleotides from the IRE; mutation showed that TBP enhance negative control.

Structure analysis of the ferritin IRE (wild type and mutant) by nuclease cleavage, alkylation, and cleavage by transition metal complexes showed: a hairpin with higher order folding [Fe-EDTA and NMR-^{1}H (pcp and 1 -1) and ^{31}-P], a G-C pair in the HL (nuclease, alkylation, NMR) and heat stable, subdomains (1,10-phen-Cu, Fe-bleomycin, Rh(phen)$_2$Phi^{3+}, NMR, UV-vis). The IRE forms the IRP binding site ("footprint"). G/A mutation in the HL abolished IRP binding and negative, but not positive control. The mutant hairpin melted 10° lower (42°), indicating the importance of the HL in stabilizing the three dimensional shape required to recognize the IRP (part support NIH-DK 20251).